AD NUMBER

ADB016383

LIMITATION CHANGES

TO:

Approved for public release; distribution is unlimited.

FROM:

Distribution authorized to U.S. Gov't. agencies only; Proprietary Information; SEP 1975. Other requests shall be referred to Department of Defense, Attn: Public Affairs Office, Washington, DC 20301.

AUTHORITY

GE DoD ltr 4 May 1977

(2) (5)

(6) CHARACTERISTICS OF HF RADAR-OVERDENSE METEOR ECHOES.

(14) R75EMH2

(10) George H. Millman

(9) Technical information series,

(11) Sept[redacted]1975

(12) 67 p.

General Electric Company HMED
Syracuse, New York 13201

GENERAL ELECTRIC COMPANY TECHNICAL INFORMATION

Within the limitations imposed by Government data export regulations and security classifications, the availability of General Electric Company technical information is regulated by the following classifications in order to safeguard proprietary information:

CLASS 1: GENERAL INFORMATION

Available to anyone on request.
Patent, legal and commercial review required before issue.

CLASS 2: GENERAL COMPANY INFORMATION

Available to any General Electric Company employee on request.
Available to any General Electric Subsidiary or Licensee subject to existing agreements.
Disclosure outside General Electric Company requires approval of originating component.

CLASS 3: LIMITED AVAILABILITY INFORMATION

Original Distribution to those individuals with specific need for information.
Subsequent Company availability requires originating component approval.
Disclosure outside General Electric Company requires approval of originating component.

CLASS 4: HIGHLY RESTRICTED DISTRIBUTION

Original distribution to those individuals personally responsible for the Company's interests in the subject.
Copies serially numbered, assigned and recorded by name.
Material content, and knowledge of existence, restricted to copy holder.

GOVERNMENT SECURITY CLASSIFICATIONS, when required, take precedence in the handling of the material. Wherever not specifically disallowed, the General Electric classifications should also be included in order to obtain proper handling routines.

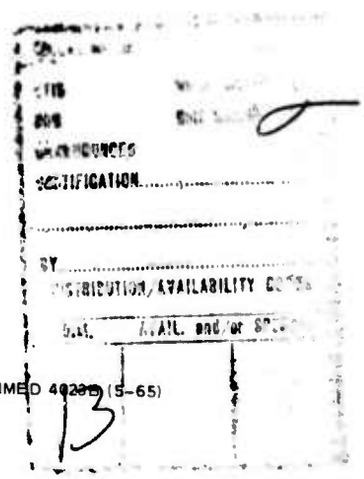

GENERAL ELECTRIC

HEAVY MILITARY EQUIPMENT DEPARTMENT

TECHNICAL INFORMATION SERIES

9 Feb 77

Author	Subject Category	No. R75EMH2
G. H. Millman	HF Radar, Overdense Meteors	Date Sept 1975

Title

CHARACTERISTICS OF HF RADAR-OVERDENSE METEOR ECHOES

~~Copies Available at:~~ HMED TIS Distribution Center ~~Box 1122~~ (CSP4) ~~Lobby~~ Syracuse, New York 13201	GE Class 1	No. of Pages 73
	Govt Class Unclassified	

Summary

The characteristics of HF radar reflections from overdense meteor ionization trails having line densities greater than 10^{14} electrons/m, are discussed. Theoretical estimates are made of the radar cross-sectional area, time duration and the doppler frequency shift of meteor echoes. Utilizing experimental meteor data recorded at 32 MHz by Greenhow and Watkins (1964), extrapolations are made of the statistical variations of the cross-sectional area, the echo duration and the meteor echo rate for frequencies in the 6-MHz to 40-MHz band.

10 to the 14th power

Key Words

HF Radar
Meteors
HF Propagation
Ionosphere

ABSTRACT

Send to _____

GENERAL ELECTRIC COMPANY
HEAVY MILITARY EQUIPMENT DEPARTMENT
TECHNICAL INFORMATION SERIES

SECTION Advanced Systems and Technology

UNIT 570

HMED ACCOUNTING REFERENCE

COLLABORATORS

APPROVED M. A. Johnson TITLE Mgr., AS&T LOCATION CSP 4-58

TIS R75EMH2

MINIMUM DISTRIBUTION - Government Unclassified Materiol (and Title Pages) in G.E. Classes 1, 2, or 3 will be the following.

Copies	Title Page Only	To
0	1	Legal Section, HMED (Syracuse)
0	1	Manager, Technological Planning, HMED (Syracuse)
5	6	G-E Technical Data Center (Schenectady)

MINIMUM DISTRIBUTION - Government Classified Materiol, Secret or Confidential in G.E. Classes 1, 2, or 3 will be the following.

1	1	Classified Section, Electronics Park Library
1	0	Manager, Technological Planning, HMED (Syracuse)

ADDITIONAL DISTRIBUTION (Keep at minimum within intent of assigned G.E. Class.)

COPIES	NAME	LOCATION
5 (CLASS 1 ONLY)	DEFENSE DOCUMENTATION CENTER	CAMERON STATION, ALEXANDRIA, VA. 22314

TABLE OF CONTENTS

LIST OF ILLUSTRATIONS

LIST OF ILLUSTRATIONS (Cont)

LIST OF TABLES

SECTION I

INTRODUCTION

Meteoric particles on entering the earth's atmosphere produce incandescence and an ionization trail extending along the path of the meteor at altitudes between approximately 80 and 120 km.

Radar echo returns from meteor trails can give rise to false targets which, in turn, could result in a serious clutter problem. For extremely high-powered radars, meteor echoes can be received in the sidelobes as well as in the main antenna beam.

In this report, the characteristics of HF radar echoes from high density (overdense) ionization trails, i.e., line density is greater than 10^{14} electrons/m, are discussed.

Theoretical estimates are made of the radar cross section and the time duration of overdense meteor echoes utilizing the theoretical models hypothesized by Eshleman (1955, 1957). The doppler frequency shifts of meteor echoes imposed by ionospheric winds are also evaluated.

From the radar-meteor observations at 32-MHz by Greenhow and Watkins (1964), an extrapolation is made of the cross-sectional area, time duration and meteor echo rate for frequencies in the HF band.

SECTION II

THEORETICAL CONSIDERATIONS

2.1 RADAR CROSS SECTION

Radar pulses backscattered from meteoric ionization are aspect sensitive in that the maximum intensities are returned when the direction of propagation is orthogonal to the trail. The reflection process is assumed to take place at the surface of the ionization trail where the condition of critical reflection is satisfied, i.e., the frequency of the incident radiation is equal to the plasma frequency of the trail.

According to Eshleman's et al. (1957) scattering theory, the maximum backscattering cross-sectional area at the long wavelengths ($\lambda > 3$ m) is given by

$$\sigma_{o\ell}\,(\max) = \left(\frac{\sigma_e}{4\pi}\right)^{1/4} q^{1/2} \lambda\, R_o\, e^{-1/2} \tag{2-1}$$

where σ_e is the radar cross section of an electron (10^{-28} m^2), q is the line density (in electrons/m, λ is the wavelength (in m) and R_o is the perpendicular distance from the radar to the meteor trail (in m).

Figure 2-1 is a plot of the radar cross section of overdense meteor trails as a function of elevation angles for frequencies in the HF band, the calculations being based on an assumed $q = 10^{14}$ electrons/m and meteor altitude of 95 km. It is seen that, for propagation along the horizon, the cross section varies between approximately 2.6×10^6 m^2 and 1.7×10^7 m^2 at 40 MHz and 6 MHz, respectively, and that, the cross section decreases by an order of magnitude at an elevation angle of 70°.

2.2 TIME DURATION

According to Eshleman (1955), assuming that the meteor trail is an infinitely long right circular cylinder and that the column of electrons expands by normal diffusion in a Gaussian distribution, the amplitude-time dependency of a reflected signal at the long wavelengths is of the form

$$A^2 = A_o^2 \left[t\, \ell n \frac{\lambda^2 q\, \sigma_e^{1/2}}{8\pi^{5/2} Dt} \right]^{1/2} \tag{2-2}$$

where A_o is the maximum amplitude and D is the ambipolar diffusion coefficient (in m^2/s).

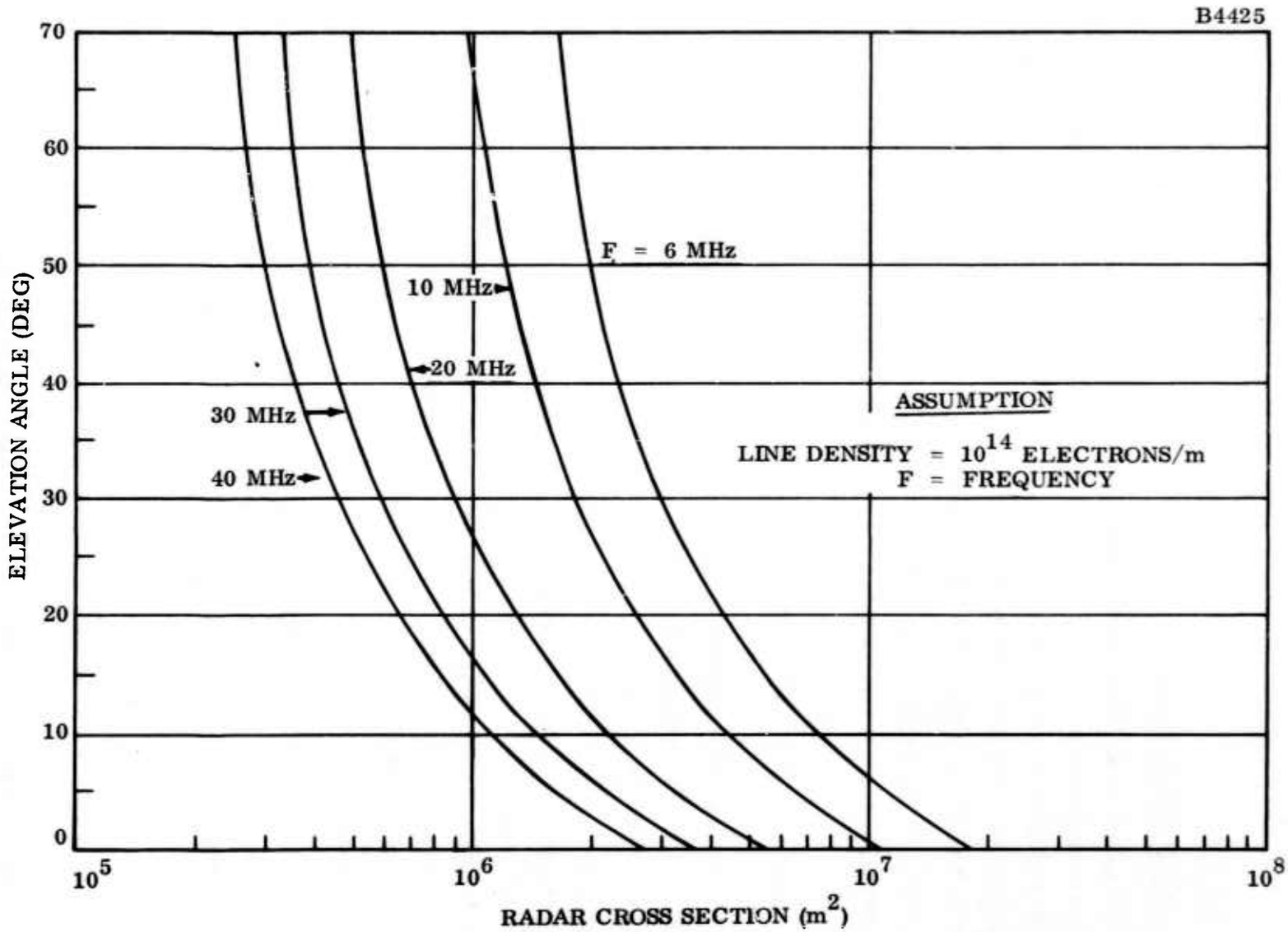

Figure 2-1. Overdense Meteor Cross Section at an Altitude of 95 km

As shown in Figure 2-2, the radar cross section, i.e., signal amplitude, increases with time to a maximum value and then decreases to zero.

The time duration of overdense meteor trails is simply the total duration of the echo and is given by

$$\tau_{o\ell} = \frac{\lambda^2 \, q \, \sigma_e^{1/2}}{8\pi^{5/2} \, D} \tag{2-3}$$

The estimates of the time durations as a function of altitude, presented in Figure 2-3, are based on Greenhow's and Neufeld's (1955) model for the ambipolar diffusion coefficient which is expressed by

$$\log_{10} D = 0.0679h - 5.663 \tag{2-4}$$

where h is the altitude of the meteor column (in km).

It is evident that the meteor echo duration increases with decreasing altitude and increasing line density. For an ionization altitude of 95 km and line density of 10^{14} electrons/m, the duration of overdense meteor echoes at 6 MHz evaluates to 2.9 s while, at 40 MHz, it decreases to about 0.66 s.

2.3 DOPPLER FREQUENCY SHIFT

The doppler frequency shift encountered by radio waves incident on meteoric ionization is mainly due to the wind motions in the ionosphere.

Assuming that, at a given altitude, the ionospheric wind velocity is Rayleigh distributed and the angular orientation of the wind in a plane parallel to the tangent plane at the earth's surface is uniformly distributed, it follows that the probability density function of the doppler frequency shift is Gaussian with a mean doppler of zero.

It can be readily shown that the standard deviation, σ, of the Gaussian distributed doppler frequency shift can be expressed by

$$\sigma = 2\left(\frac{2}{\pi}\right)^{1/2} \frac{\bar{V}}{\lambda} \left(\frac{r_o}{r_o + h}\right) \cos E \tag{2-5}$$

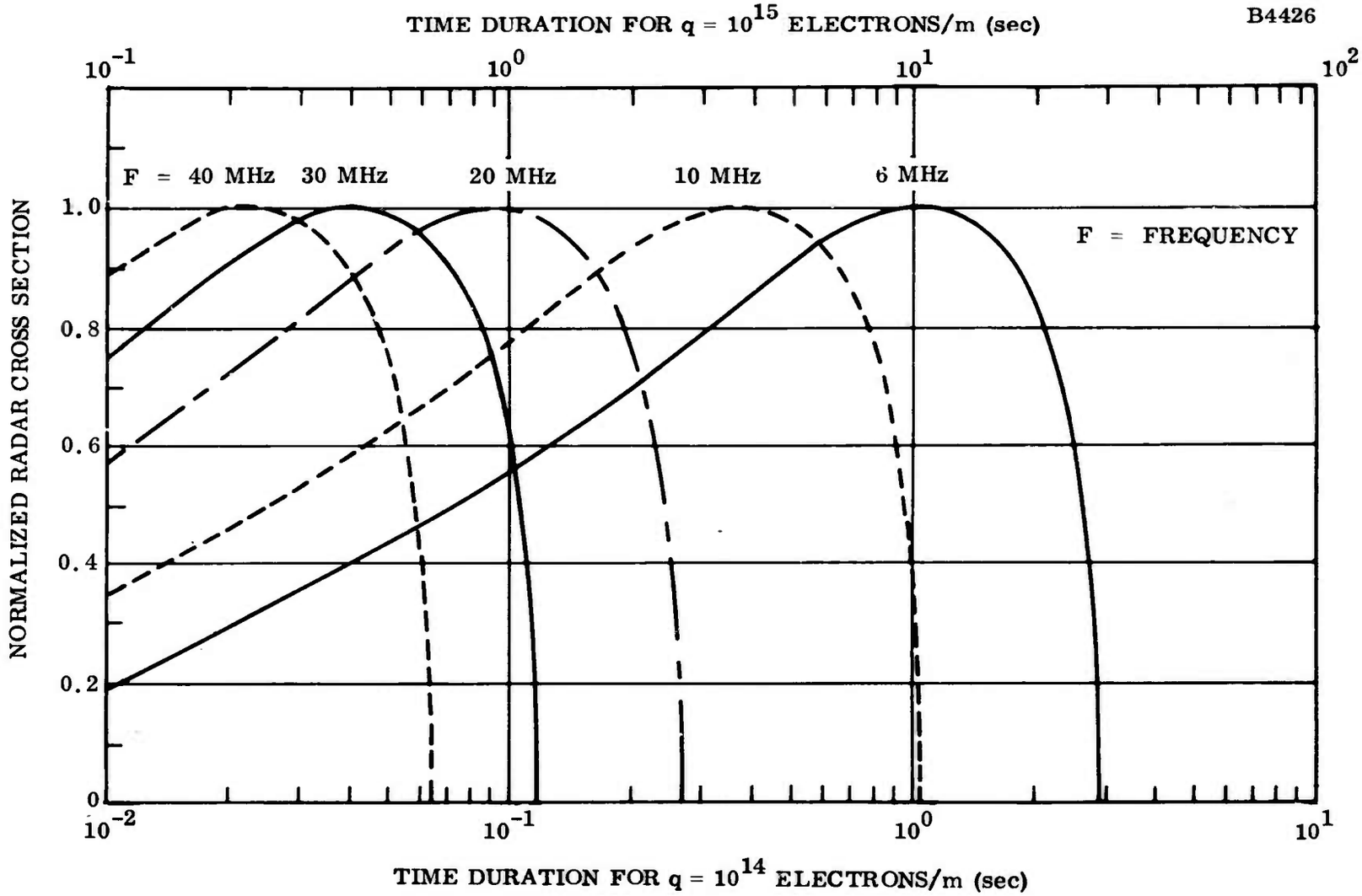

Figure 2-2. Normalized Radar Cross Section of Overdense Meteors as a Function of Time Duration for an Ionization Altitude of 95 km

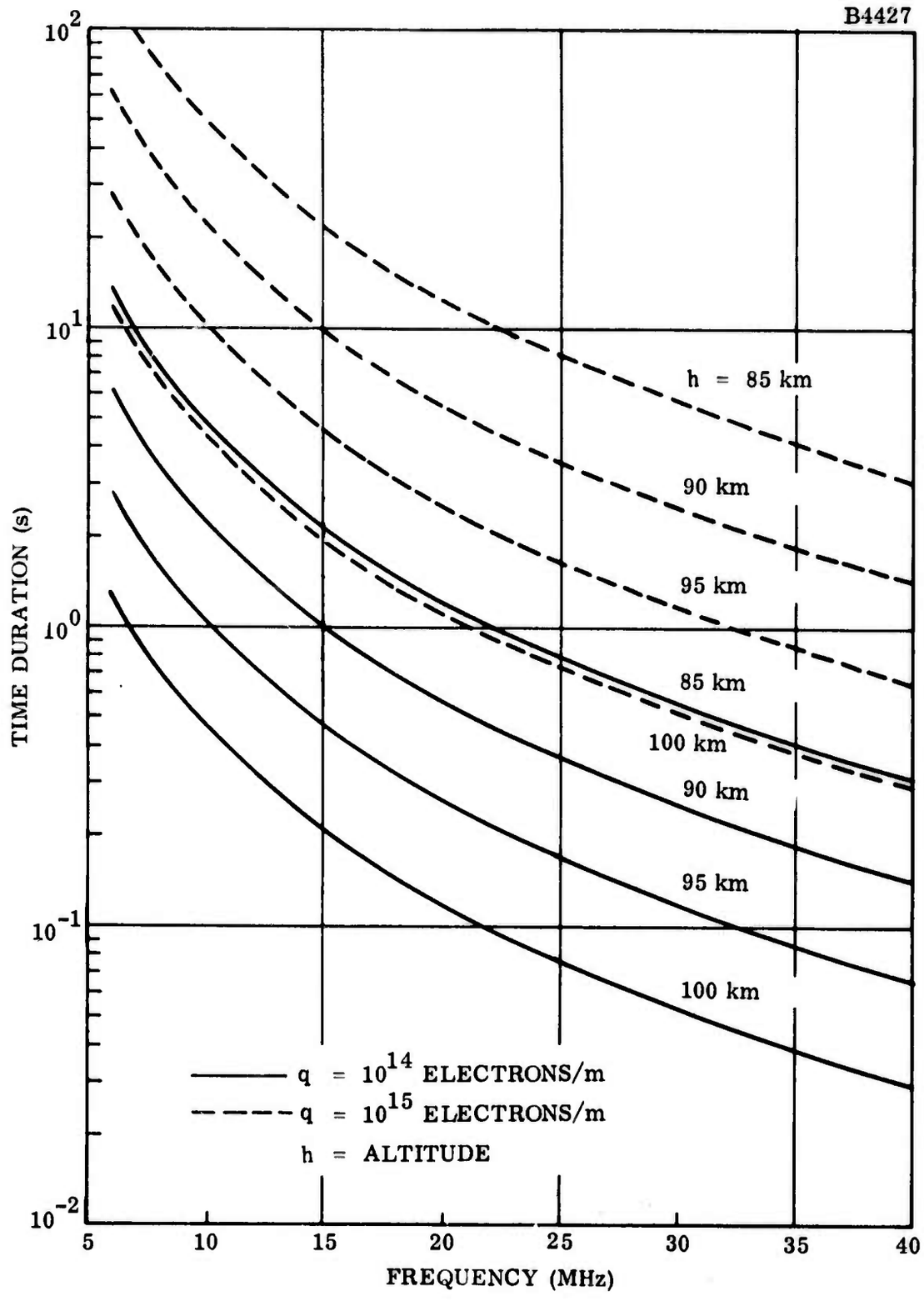

Figure 2-3. Time Duration of Overdense Meteor Trail Echoes at HF

where $\overline{V}$ is the mean wind velocity, r_o is the earth's radius (6371 km), h is the meteor ionization altitude, and E is the elevation angle to the meteor trail as measured from the horizon. The derivation of this relationship is presented in Appendix A.

The estimated standard deviation and the upper decile ($\approx 1.28\sigma$) of the doppler frequency shifts at 6 MHz and 40 MHz for winds at 95 km altitude are shown in Figures 2-4 and 2-5, respectively. The statistical distribution of the mean ionospheric wind velocity was deduced from the experimental measurements summarized by Rao (1965).

According to Figure 2-4, at 6 MHz, the upper decile doppler frequency shift imposed by ionospheric winds having a mean-median velocity of 80 m/s could vary between approximately 3.0 and 3.2 Hz for elevation angles less than 20°. At 40 MHz, the doppler frequency shift, for the same conditions, varies between 20.0 and 21.3 Hz.

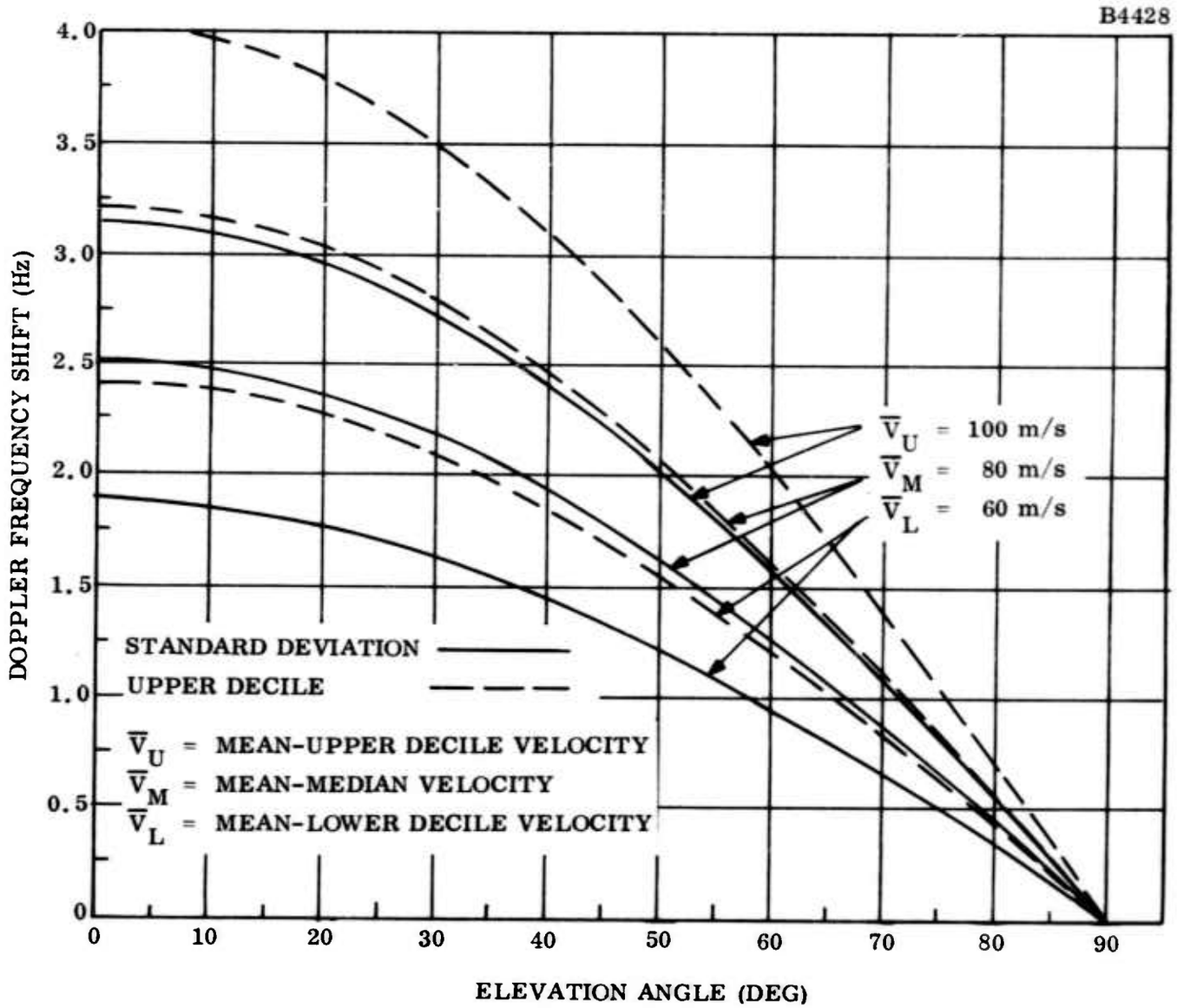

Figure 2-4. Distribution of Meteor Trail Doppler Frequency Shifts as a Function of Elevation Angle and Ionospheric Wind Speeds of 6 MHz

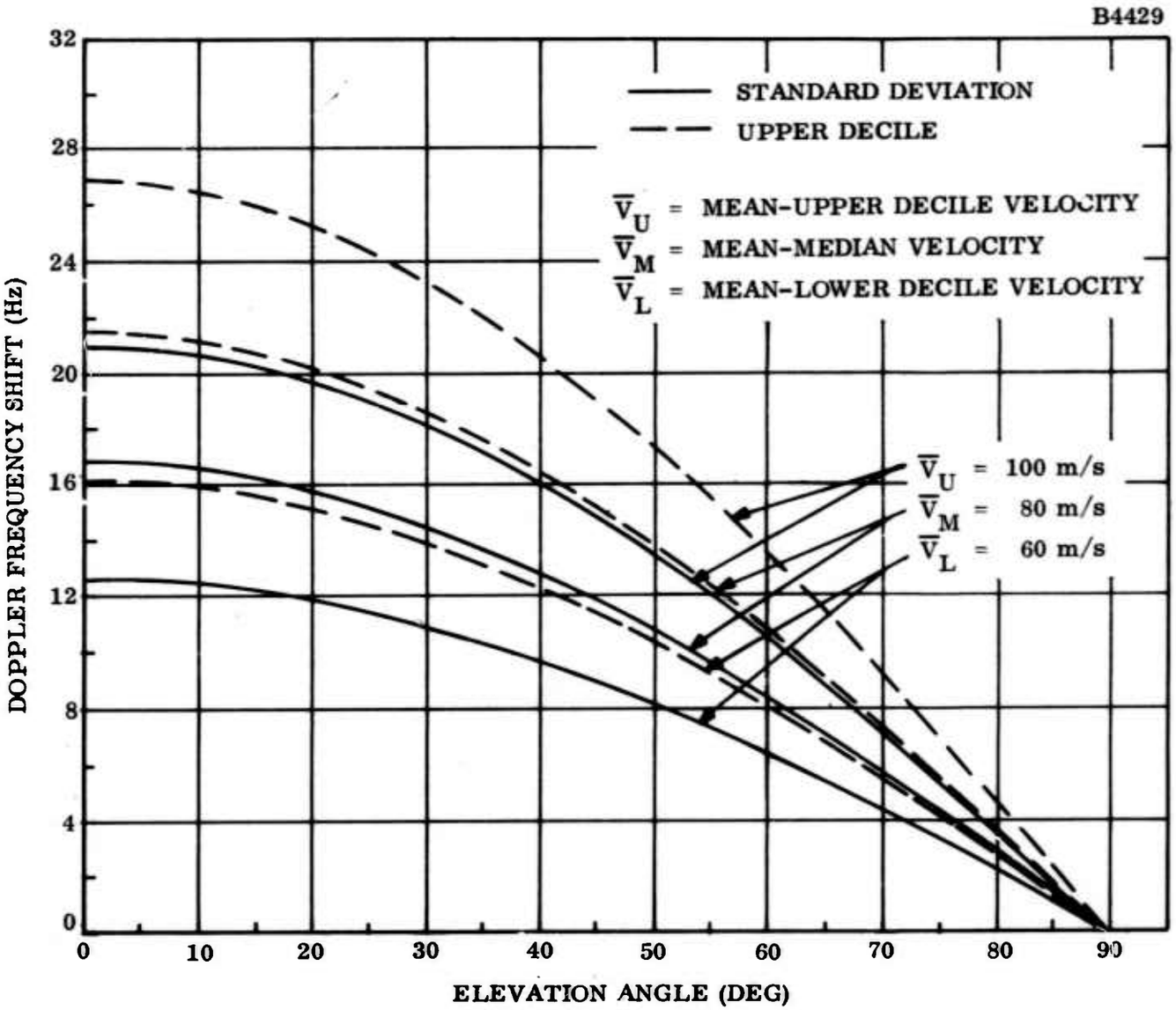

Figure 2-5. Distribution of Meteor Trail Doppler Frequency Shifts as a Function of Elevation Angle and Ionospheric Wind Speeds at 40 MHz

SECTION III

EXPERIMENTAL MEASUREMENTS

3.1 SYSTEM PARAMETERS

A study of radar reflections at 32 MHz conducted by Greenhow and Watkins (1964) in England in the fall of 1961 can be directly applied for estimating the characteristics of meteor echoes at other frequencies in the HF band. Radar meteor observations were also made at a frequency of 300 MHz, the 32 MHz data being used to assist in the interpretation of echoes occurring simultaneously at the higher frequency.

The parameters of the HF radar equipment used in the Greenhow-Watkins experiment are given in Table 3-1. The meteor data were collected with the antenna oriented at a fixed azimuth of 30° east of north and at an elevation angle of 10°.

TABLE 3-1
GREENHOW'S AND WATKINS' RADAR PARAMETERS

Frequency	32 MHz
Transmitter Peak Power	7 kW
Pulse Length	140 μs
Pulse Repetition Frequency	50 pulses/s
Antenna Diameter	25 m
Antenna Beamwidth	25°
Antenna Gain	16 dB
Cosmic Noise	15,000°K

3.2 EXPERIMENTAL RESULTS

Figure 3-1 is a plot of the mean heights of the 300-MHz echoes as a function of the duration time of the coincident 32-MHz echoes and the approximate values of the meteor trail line density. It is seen that the line density increases as the mean height increases which is contrary to meteor theory (Greenhow, 1963).

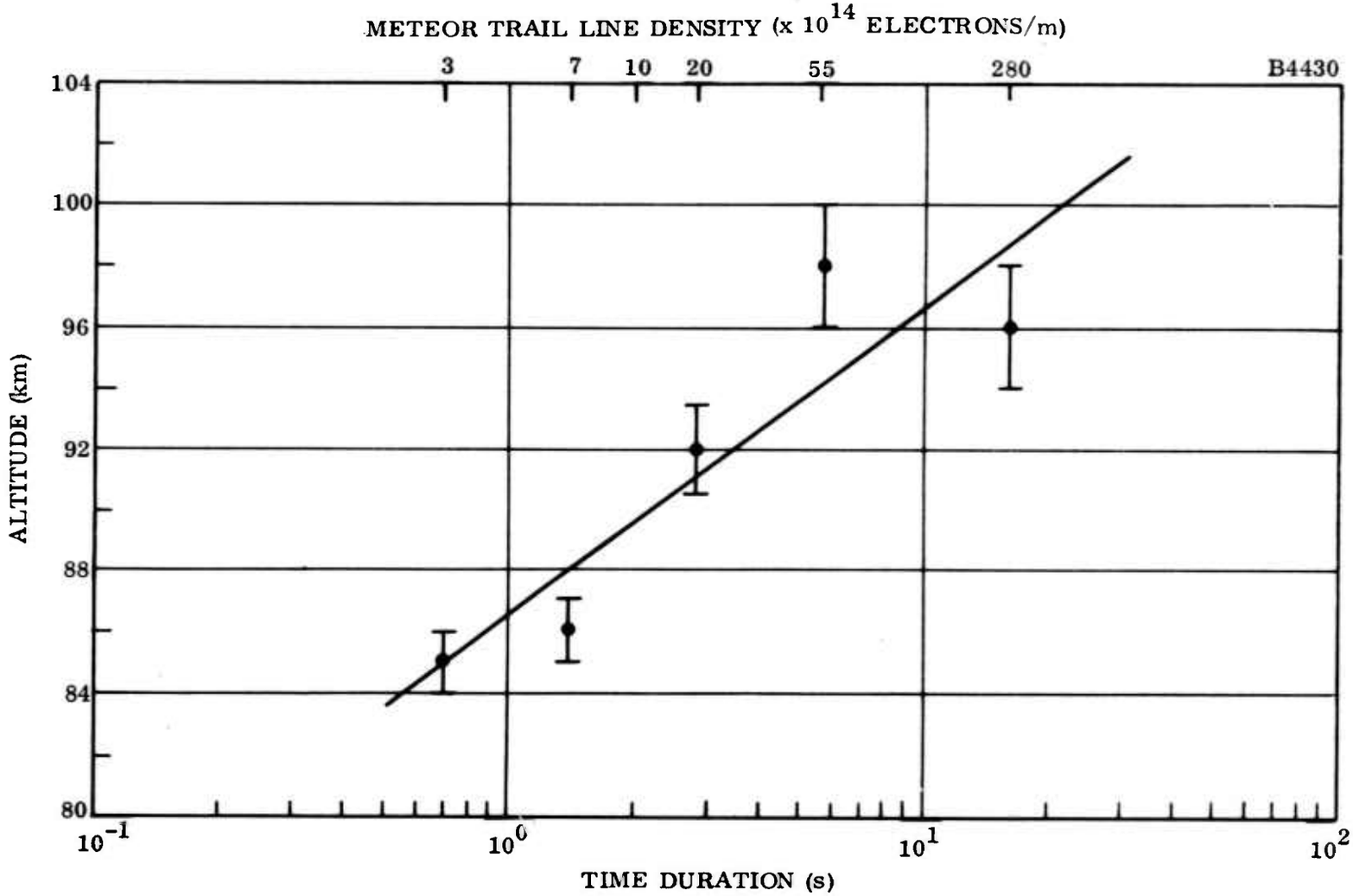

Figure 3-1. Mean Heights of 300-MHz Echoes as a Function of the Time Duration of the Coincident 32-MHz Echoes and the Approximate Values of the Meteor Trail Line Density (After Greenhow and Watkins, 1964)

According to Equation (2-3), the line density is directly proportional to the duration time. However, as shown in Figure 3-2, there is a slight deviation of the line density-duration time plot from a linear fit. This deviation is most likely due to the fact that the data are based on meteor echoes recorded at all altitudes and that the diffusion coefficient, which appears in Equation (2-3), is altitude dependent.

The meteor cross-sectional area presented in Figures 3-3 and 3-4 as a function of line density and echo duration, respectively, was calculated utilizing Equation (2-1) with the mean altitude data of Figure 3-1.

A histogram of the echo duration of the 32-MHz echoes which correlated with the 300-MHz echoes is given in Figure 3-5.

The integration of the area under the histogram of Figure 3-5 results in the cumulative distribution function of echo duration shown in Figure 3-6. Utilizing Figure 3-6 in conjunction with Figures 3-2 and 3-4, it follows that the cumulative distribution function of line density and cross-sectional area can be readily derived. A summary of the statistical characteristics, i.e., lower decile, lower quartile, median, upper quartile and upper decile, of the echo duration, line density and cross sectional area, as obtained from Figures 3-6, 3-7 and 3-8, respectively, are summarized in Table 3-2.

Figure 3-9 is a plot of the diurnal variation of the meteor rate for echoes with time durations greater than 1 s. It is seen that the rate is a maximum of about 235 meteors/h in the early hours of the morning and a minimum of about 40 meteors/h in the evening.

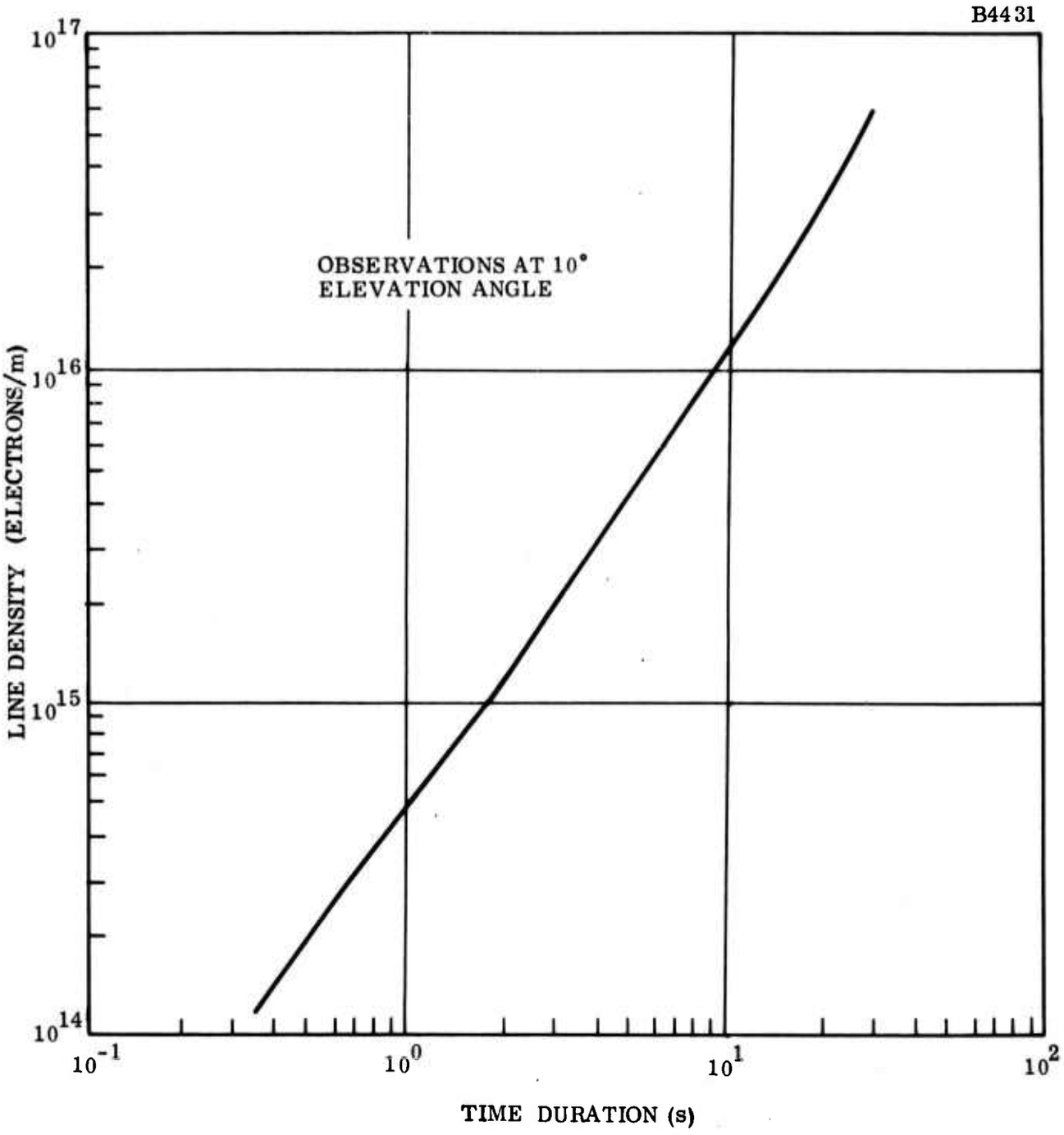

Figure 3-2. Line Density as a Function of Time Duration Based on Greenhow's and Watkins' Data (1964) at 32 MHz

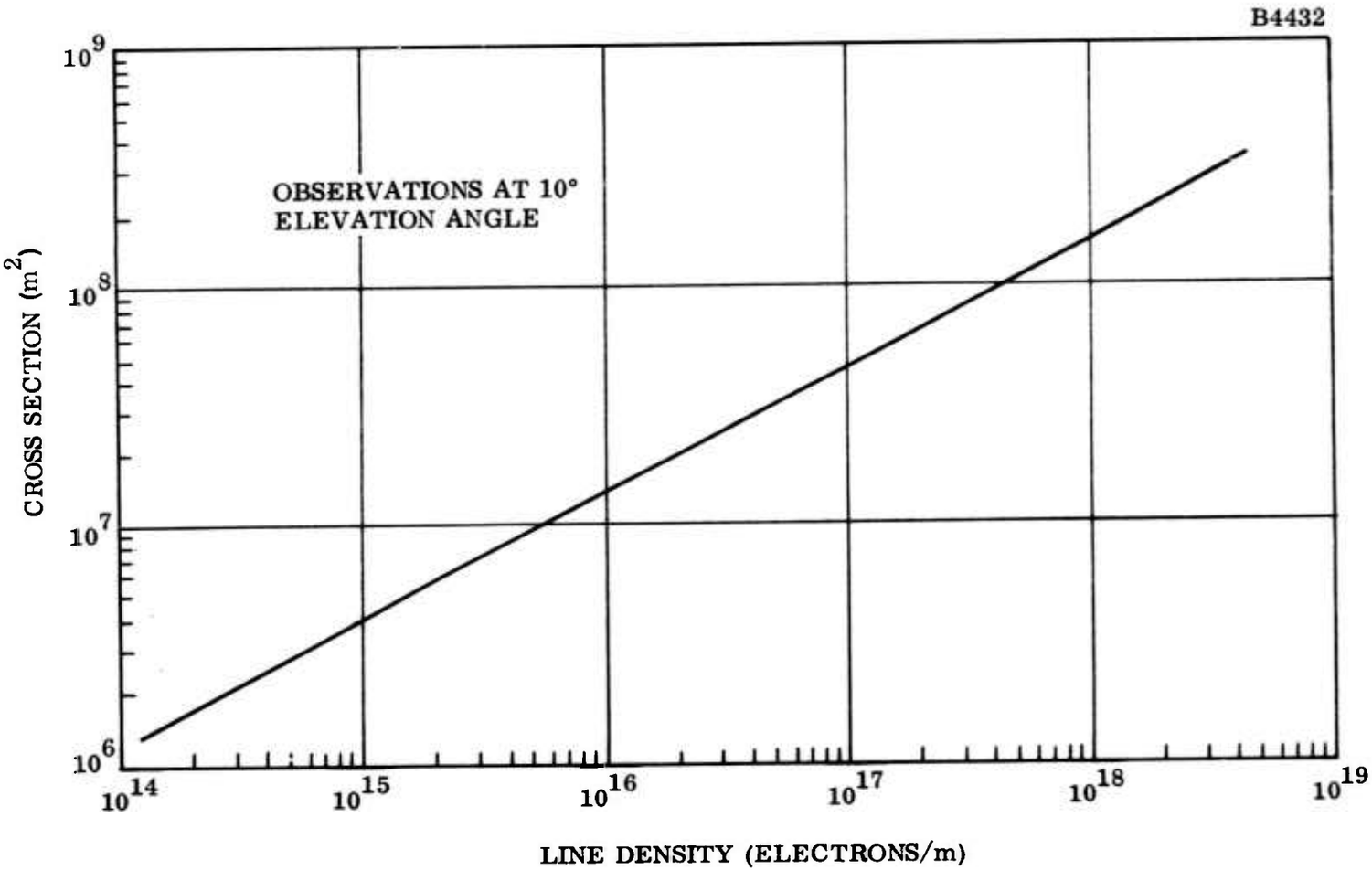

Figure 3-3. Cross Section as a Function of Line Density Based on Greenhow's and Watkins' Data (1964) at 32 MHz

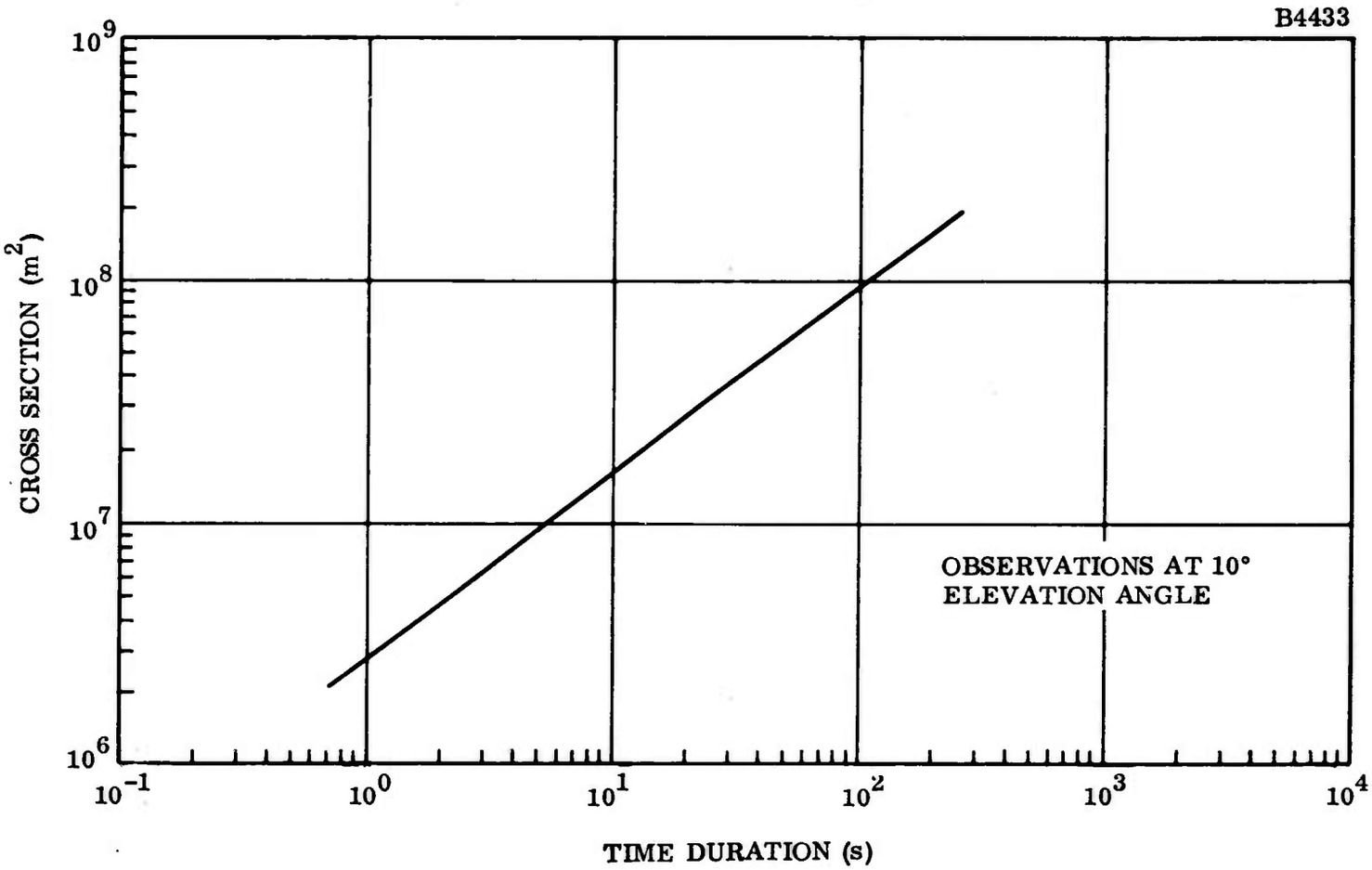

Figure 3-4. Radar Cross Section of Overdense Meteor Echoes as a Function of Time Duration Based on Greenhow's and Watkins' Data (1964) at 32 MHz

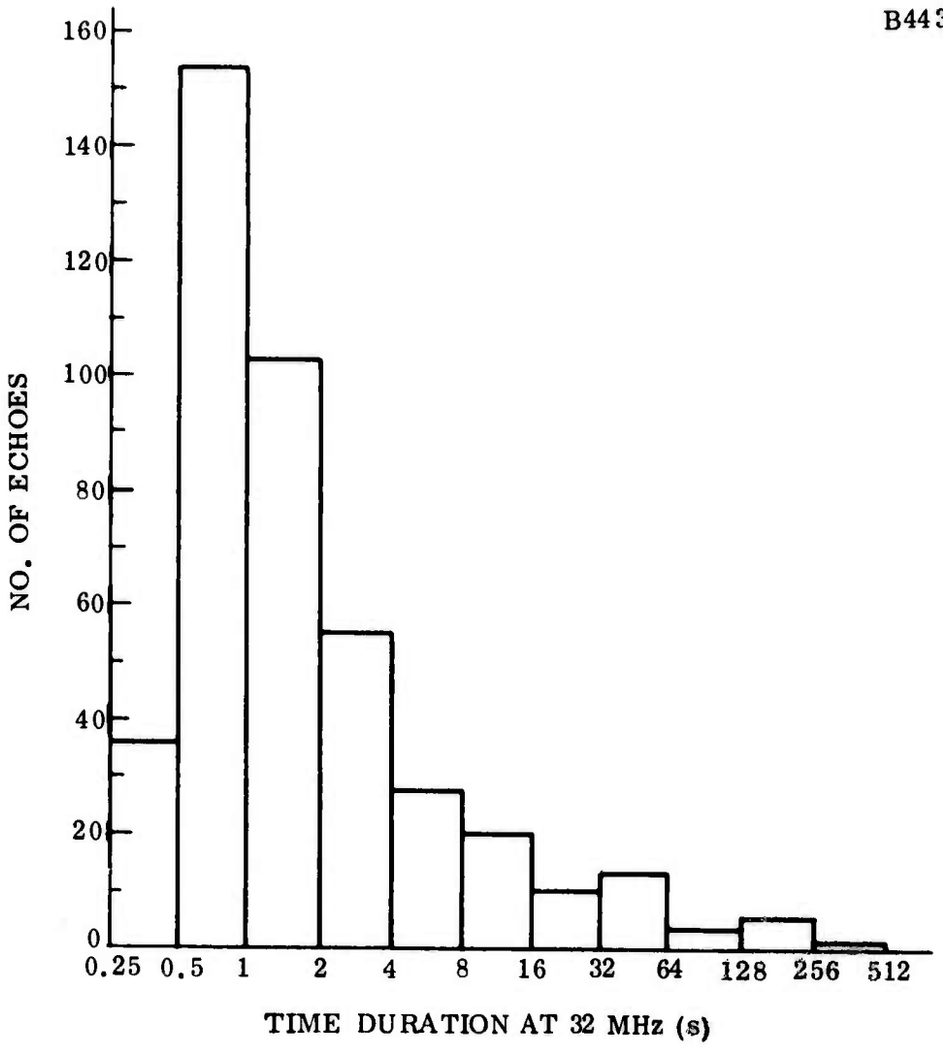

Figure 3-5. Time Duration Distribution of 32-MHz Echoes Which Correlate with 300-MHz Echoes (After Greenhow and Watkins, 1964)

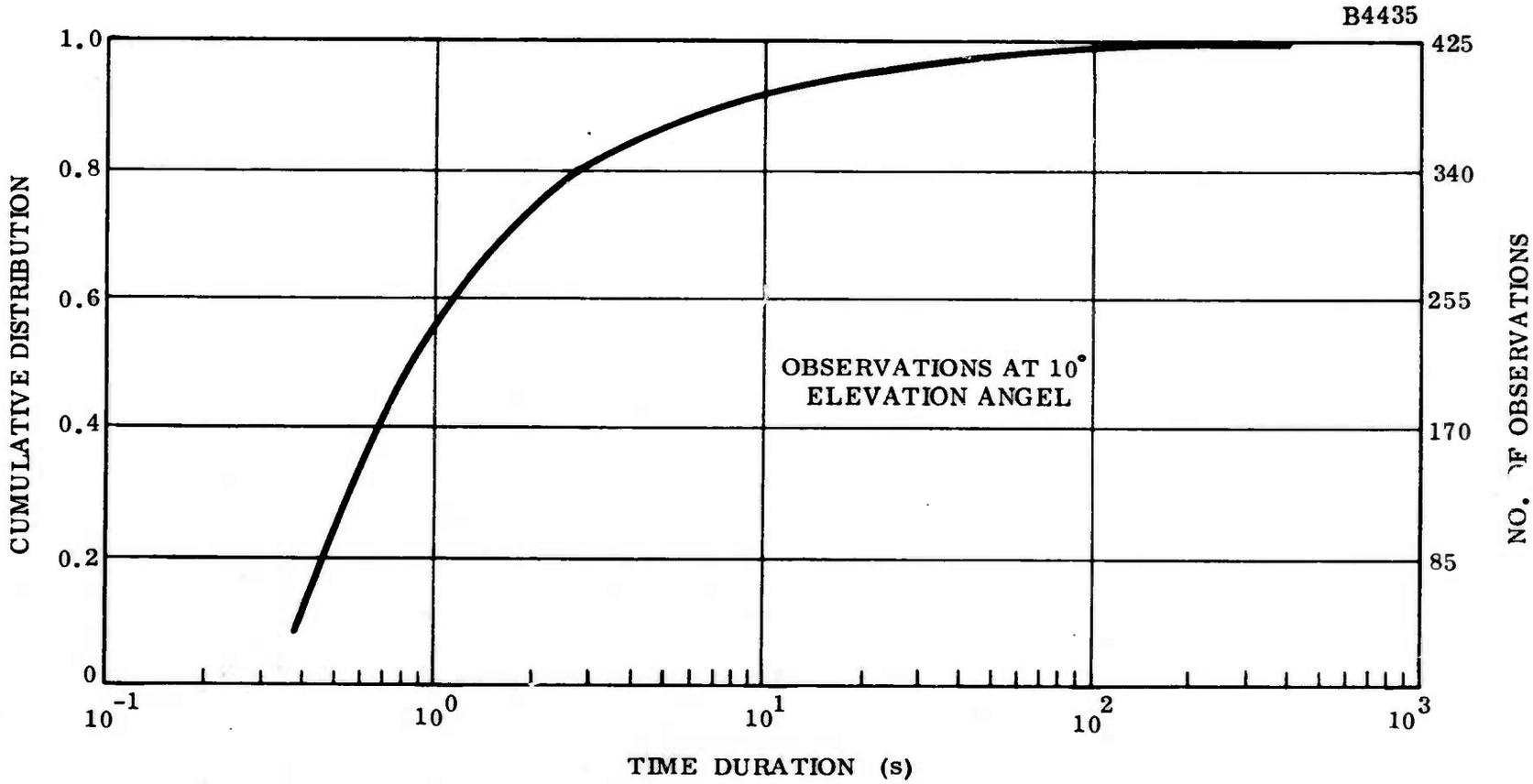

Figure 3-6. Cumulative Distribution Function of Meteor Trail Time Duration of 32-MHz Echoes Which Correlate with 300-MHz Echoes Based on Greenhow's and Watkins' Data (1964)

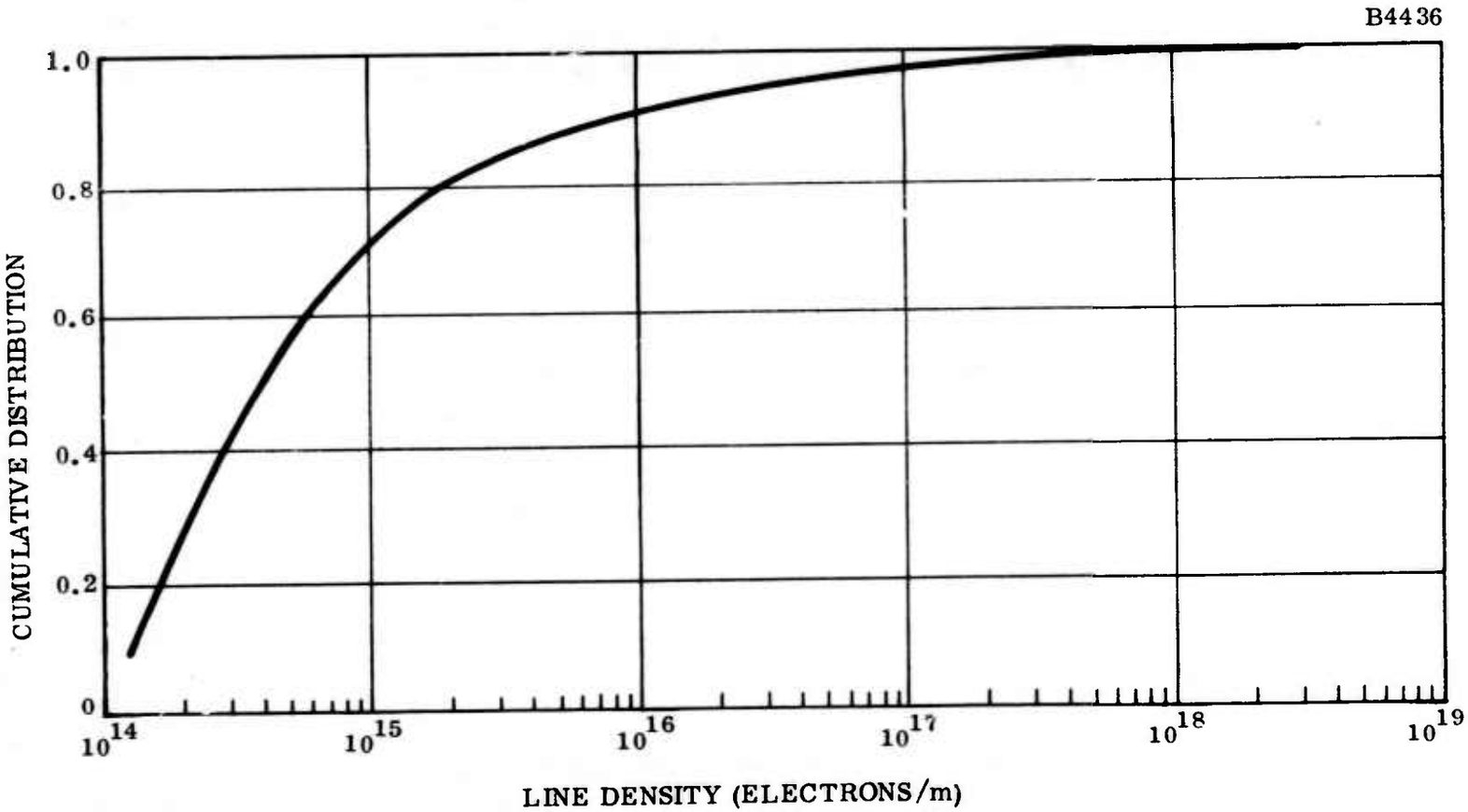

Figure 3-7. Cumulative Distribution Function of Meteor Line Density Based on Greenhow's and Watkins' Data (1964) at 32 MHz

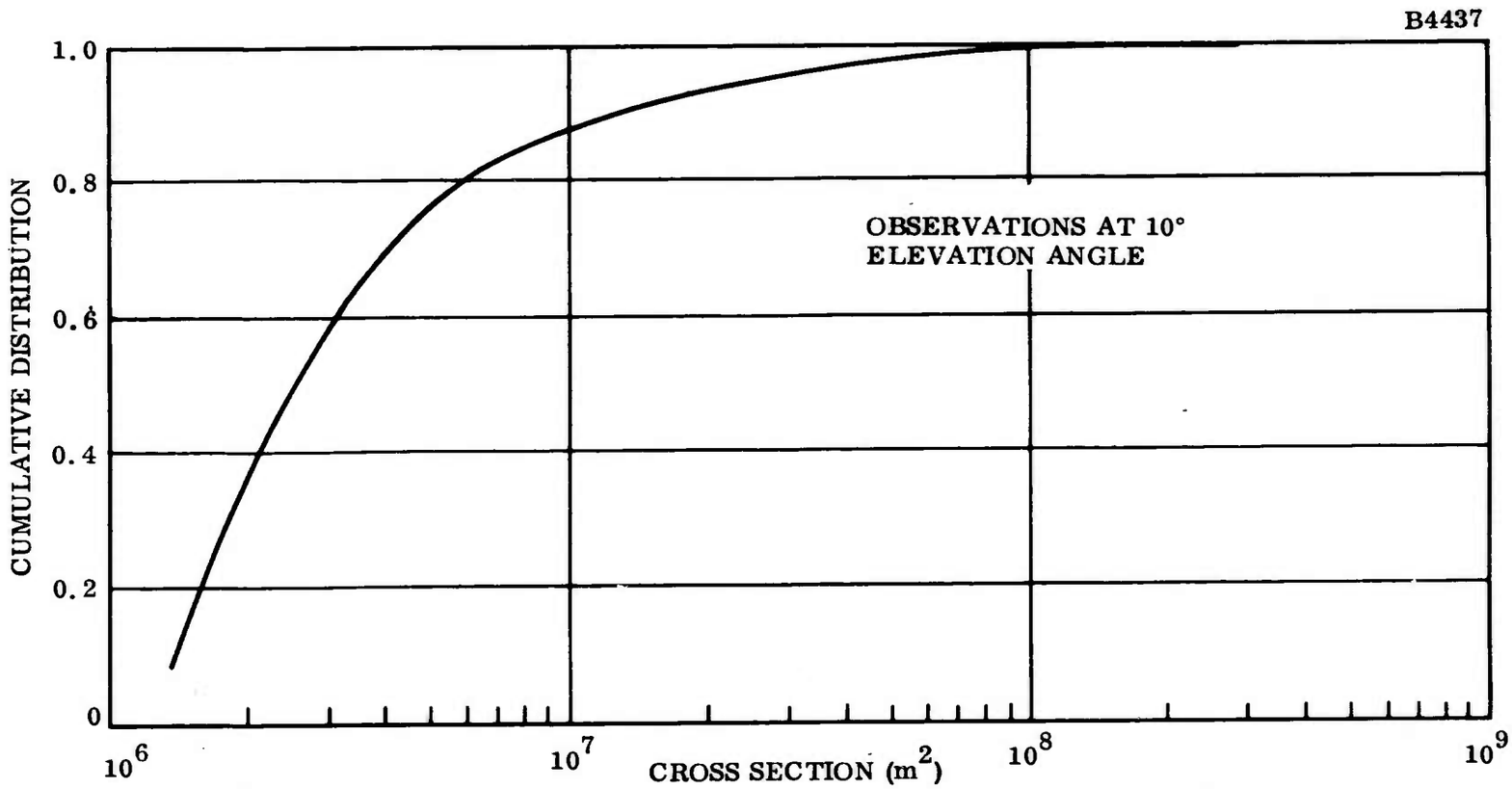

Figure 3-8. Cumulative Distribution Function of Meteor Cross Section of 32-MHz Echoes Which Correlate with 300-MHz Echoes Based on Greenhow's and Watkins' Data (1964)

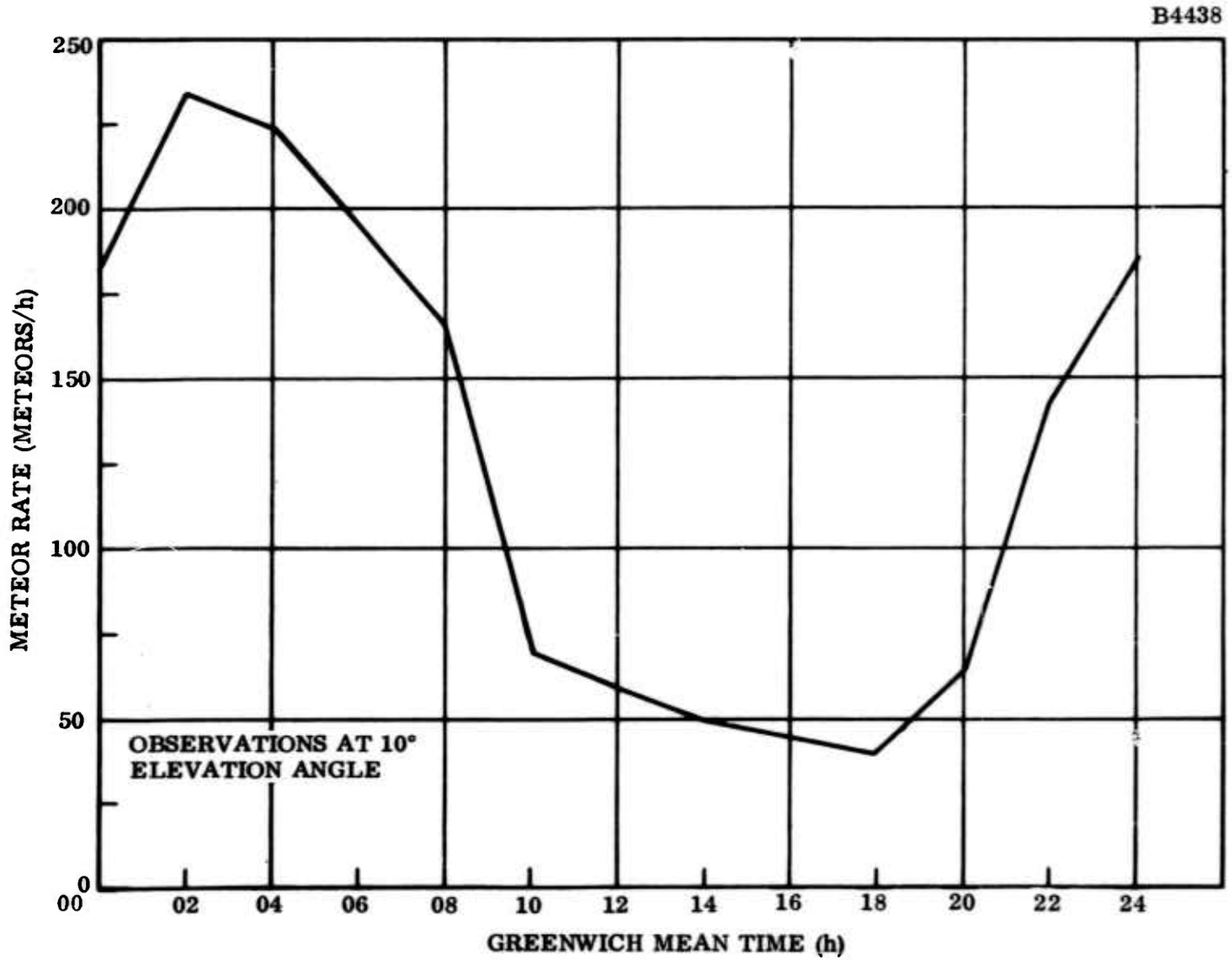

Figure 3-9. Rate of 32-MHz Echoes with Time Durations Greater than One Second (After Greenhow and Watkins, 1964)

TABLE 3-2

STATISTICAL CHARACTERISTICS OF GREENHOW'S AND WATKINS' METEOR DATA AT 32 MHz

	Echo Duration (s)	Line Density (Electrons/m)	Cross Section (m^2)
Lower Decile	0.38	1.30×10^{14}	1.38×10^{6}
Lower Quartile	0.48	1.75×10^{14}	1.63×10^{6}
Median	0.85	4.00×10^{14}	2.53×10^{6}
Upper Quartile	1.20	1.03×10^{15}	4.70×10^{6}
Upper Decile	7.50	8.60×10^{15}	1.30×10^{7}

SECTION IV

EXTRAPOLATION OF EXPERIMENTAL DATA

Greenhow's and Watkins' (1964) 32-MHz meteor data can be used as a base for predicting the characteristics of meteor echoes at other frequencies in the HF band.

According to Equations (2-1) and (2-3), the meteor cross section is inversely proportional to frequency while the time duration is inversely proportional to the square of frequency. Utilizing these relationships, it is then possible to convert the Greenhow's and Watkins' cross section and time duration results, shown in Figures 3-4, 3-6 and 3-8, to frequencies of interest. As an example, the cross section-echo duration plot of Figure 3-4 when extrapolated to frequencies between 6 MHz and 40 MHz results in Figure 4-1.

Table 4-1 contains the statistical characteristics of meteor cross section and echo duration at 6 MHz and 40 MHz as extrapolated from Greenhow's and Watkins' (1964) data. It is seen that, at the low end of the HF band, 50% of the meteor echoes could persist for times greater than about 24 s while, at the high end of the frequency band, the time durations decrease to about 0.5 s.

An examination of the system parameters given in Table 3-1 reveals that the radar employed by Greenhow and Watkins (1964) observed all the overdense meteor echoes. Although the half-power beamwidth was 25°, overdense meteors could be detected as far down as 26.15° from the antenna beam axis. This calculation which is discussed in Appendix C was based on the following assumptions: (1) the system sensitivity was set by the cosmic noise level; (2) an SNR of 10 dB was required to detect the minimum (overdense meteor) line density of 10^{14} electrons/m; (3) the circular antenna was uniformly illuminated, i.e., the amplitude and phase of the radiation across the face of the antenna aperture was uniform. The normalized one-way radiation pattern of a circular antenna is

$$S(\gamma) = 2\,\frac{J_1(\pi D \sin\gamma/\lambda)}{(\pi D \sin\gamma/\lambda)} \qquad (4\text{-}1)$$

where $J_1(\pi D \sin\gamma/\lambda)$ is the Bessel function of the first order, D is the diameter of the aperture, λ is the transmitted wavelength and γ is the angle off the beam axis.

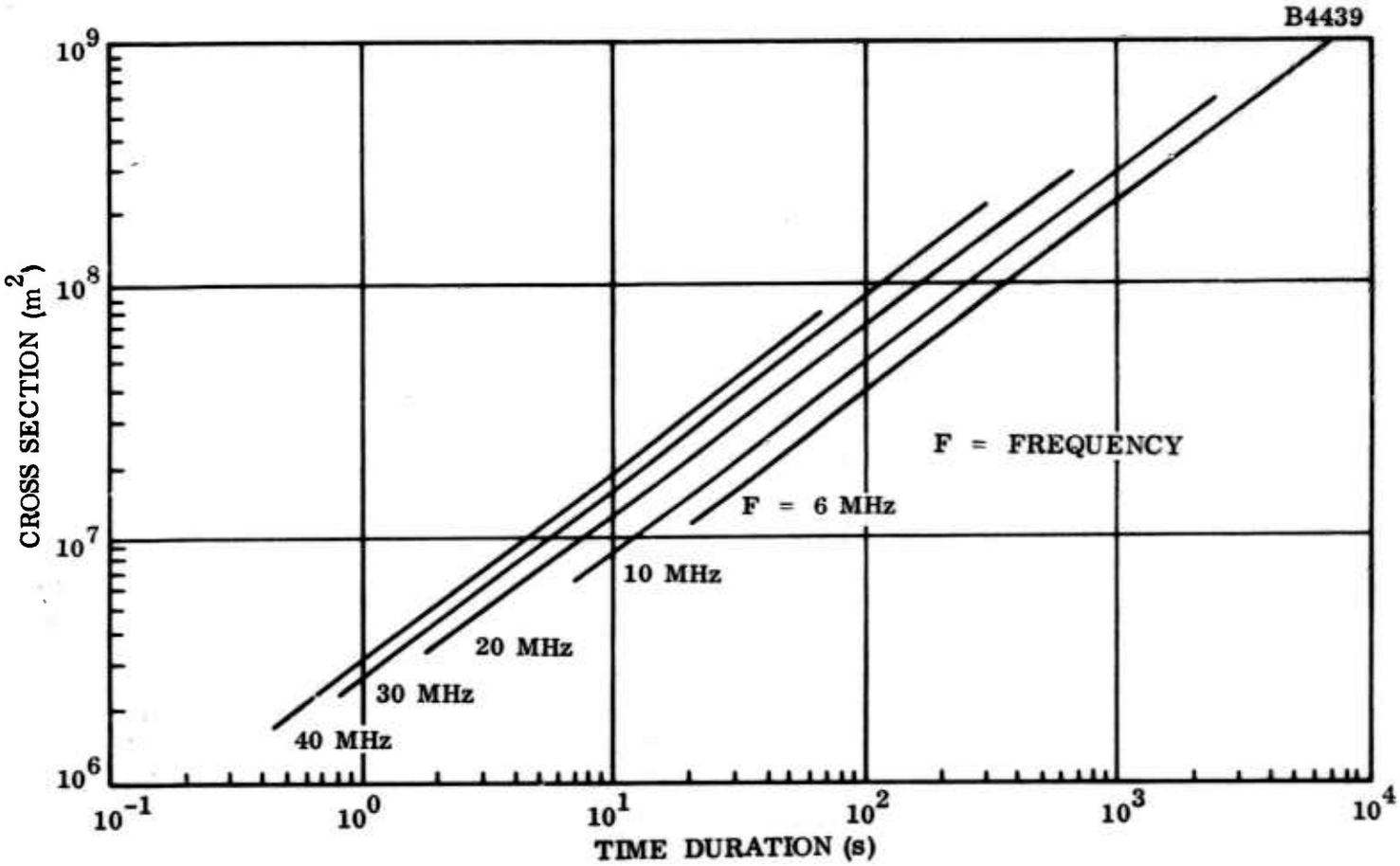

Figure 4-1. Radar Cross Section of Overdense Meteor Echoes at HF as a Function of Time Duration Extrapolated from Greenhow's and Watkins' Data (1964) at 32 MHz, 10° Elevation Angle

TABLE 4-1

CROSS-SECTIONAL AREA AND TIME DURATION OF METEOR ECHOES EXTRAPOLATED FROM GREENHOW'S AND WATKINS' DATA AT 32 MHz

Frequency	Statistics	Cross Section (m^2)	Echo Duration (s)
6 MHz	Lower Decile	7.36×10^6	10.81
	Lower Quartile	8.69×10^6	16.65
	Median	1.35×10^7	24.18
	Upper Quartile	2.51×10^7	34.13
	Upper Decile	6.93×10^7	213.33
40 MHz	Lower Decile	1.10×10^6	0.24
	Lower Quartile	1.30×10^6	0.31
	Median	2.02×10^6	0.54
	Upper Quartile	3.76×10^6	0.77
	Upper Decile	1.04×10^7	4.80

As shown in Appendix D, the area in the meteor band formed by the intersection of the (Greenhow and Watkins) antenna beam diameter of 52.3° with the 95-km altitude surface evaluates to approximately 4.20×10^5 km^2.

In deriving the overdense meteor echo rate that could be observed with a high-powered HF backscatter radar, it is necessary to determine the area in the meteor band being illuminated by the main antenna beam and sidelobes since the meteor rate is directly proportional to the area. It is assumed that the radar has sufficient sensitivity to detect meteoric ionization in the sidelobes at all elevation angles (E = 0° to 90°) and over a 180° azimuthal spread. The latter is based on the assumption that there are "holes" in the azimuth sidelobe pattern and that only one-half of the 360° azimuth angle coverage is effective in transmission and reception.

The area under illumination at an altitude of 95 km for the condition of 90° elevation angle coverage and 180° azimuth angle coverage is equal to 1.93×10^6 km^2, the computation being performed in Appendix E. It follows that an HF backscatter radar would intercept approximately 4.60 times more overdense meteors in the direct line-of-sight than detected by the Greenhow and Watkins radar.

In the operation of an HF backscatter radar, it is necessary, for the most part, to utilize the F-layer mode of propagation. Some of the overdense meteor echoes detected by reflections from the F-layer could appear in the radar range interval of the line-of-sight meteor echoes. The radar range of the F-layer reflected meteor echo will coincide with the line-of-sight meteor range for the condition in which $R \geq R_1 + R_2$ where R is the radar-horizon range to the meteor trail and R_1 and R_2 are the ranges illustrated in Figure 4-2.

In estimating the magnitude of the F-layer reflection meteor echoes appearing in the line-of-sight, it is assumed that (1) the reflections occur at an altitude of 350 km, (2) the meteor echo altitude is 95 km, and (3) the skip distance is 500 nmi (926.6 km), i.e., the minimum distance at which a ray can return to the ground after reflection from the ionosphere. As discussed in Appendix F, for these assumptions, the line-of-sight F-layer reflected echoes will be confined within the elevation angles of 30°32' and 34°13'. The latter specifies the maximum elevation angle for the F-layer mode of propagation to exist for the above assumed conditions while the former is the elevation angle which satisfies the range condition, $R = R_1 + R_2$, shown in Figure 4-2. The surface area at the meteor

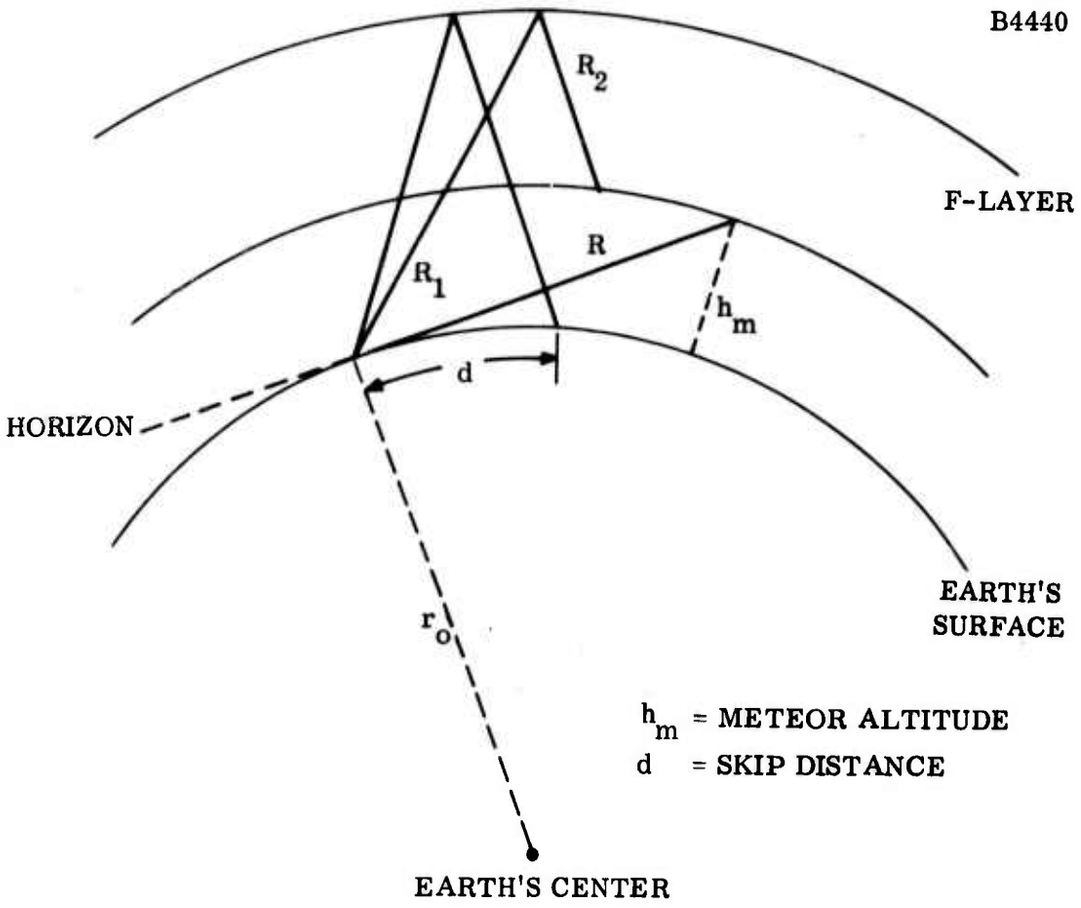

Figure 4-2. F-Layer Reflection Meteor Echo Geometry

band encompassed by the two elevation angles having an angular difference of 3°41' and the 180° azimuth spread evaluates to 2.91×10^5 km^2 which is approximately 0.69 of the surface area of 4.20×10^5 km^2 under surveillance in the Greenhow and Watkins experiment. Thus, an HF backscatter radar would observe by F-layer reflections a factor of 0.69 the number of overdense meteor echoes reported by Greenhow and Watkins and presented in Figure 3-9.

Figure 4-3 is a plot of the estimated diurnal rate of overdense meteor echoes, as extrapolated from Figure 3-9, that could be detected in the line-of-sight by both direct reflections and by F-layer reflections, the average rates being 9.4 meteors/min and 1.4 meteors/min, respectively, and the average total line-of-sight rate being 10.8 meteors/min. In addition to diurnal variations, the meteor rate will be modified by seasonal effects and meteor showers which are not considered in this analysis. The presence of meteor showers could increase the overdense meteor rate, depicted in Figure 4-3, by a factor of approximately 5 to 10.

It should be noted that, for skip distances greater than approximately 568 nmi (1052.6 km), the elevation angle defining the F-layer propagation mode for an assumed 350-km F-layer altitude would be less than 30°32'. Thus, for this case, F-layer reflected meteor echoes would not be present in the range interval of the line-of-sight meteor echoes.

According to Manning and Eshleman (1959), the average meteor flux incident on the earth's atmosphere, corresponding to line densities equal to and greater than 10^{14} electrons/m is 1.6×10^{-12} m^{-2} s^{-1}. Thus, the average overdense meteor rate observed in the direct line-of-sight and by F-layer reflections should be on the order of 185.3 meteors/min and 27.9 meteors/min, respectively. It is evident that these values are about a factor of 20 times greater than the estimates obtained using the Greenhow and Watkins data. The discrepancy in the results can most likely be attributed to the fact that Manning's and Eshleman's data do not take into account aspect sensitivity effects.

The incremental elevation angle-meteor rate in the direct line-of-sight as deduced from Greenhow's and Watkins' measurements are shown in Figures 4-4 and 4-5. The mathematical expression relating the meteor rate in terms of the incremental elevation angle is derived in Appendix G. It is interesting to note that, for the direct line-of-sight case, an insignificant amount of overdense meteor echoes should be detected at elevation angles greater than about 20° and that the number of echoes originating from F-layer reflections should be on the same order of magnitude as the total number detected above 10° elevation angle in the direct line-of-sight.

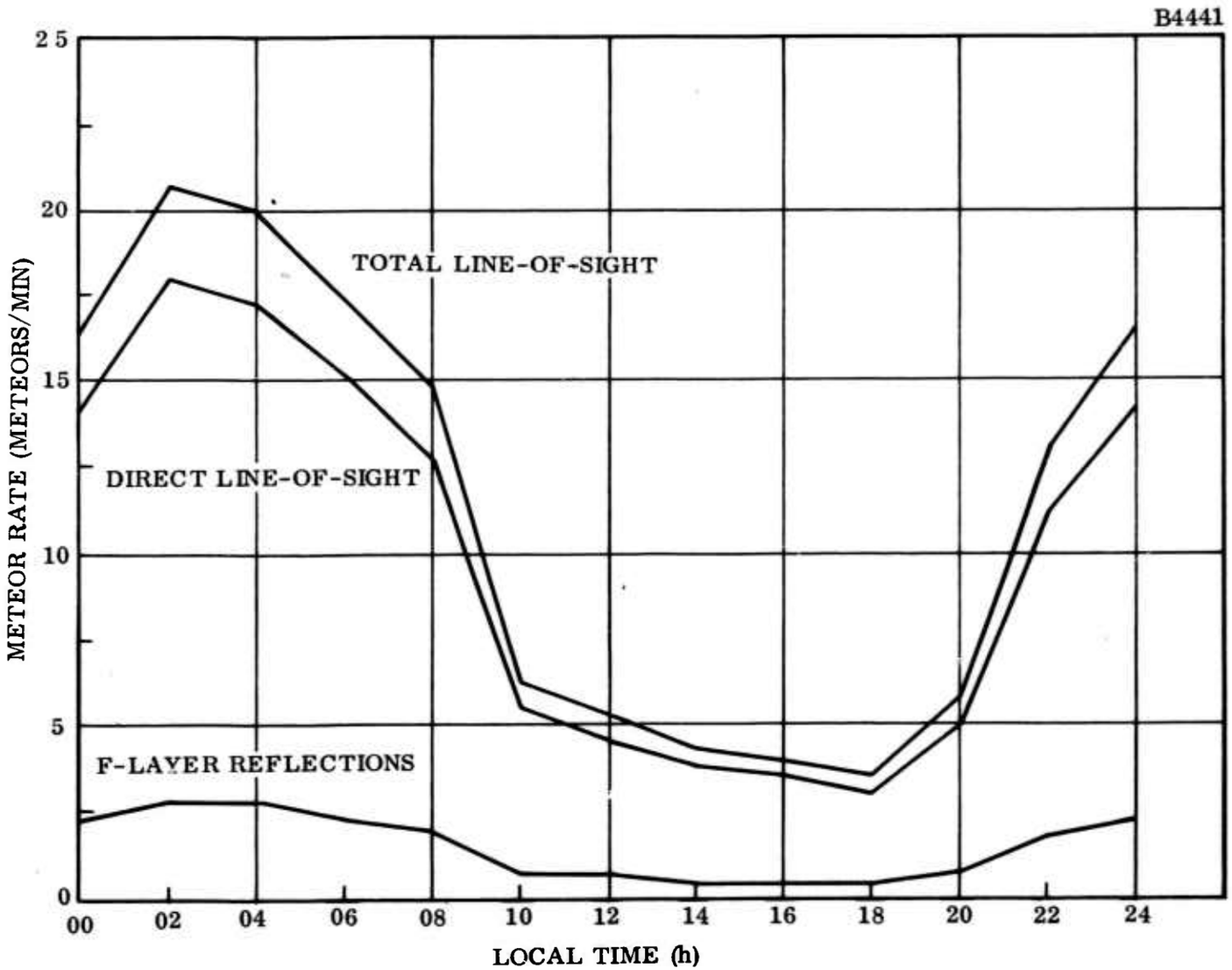

Figure 4-3. Estimated Rate of Overdense Meteor Echoes in Line-of-Sight at HF Band Based on Greenhow's and Watkins' Data (1964) at 32 MHz

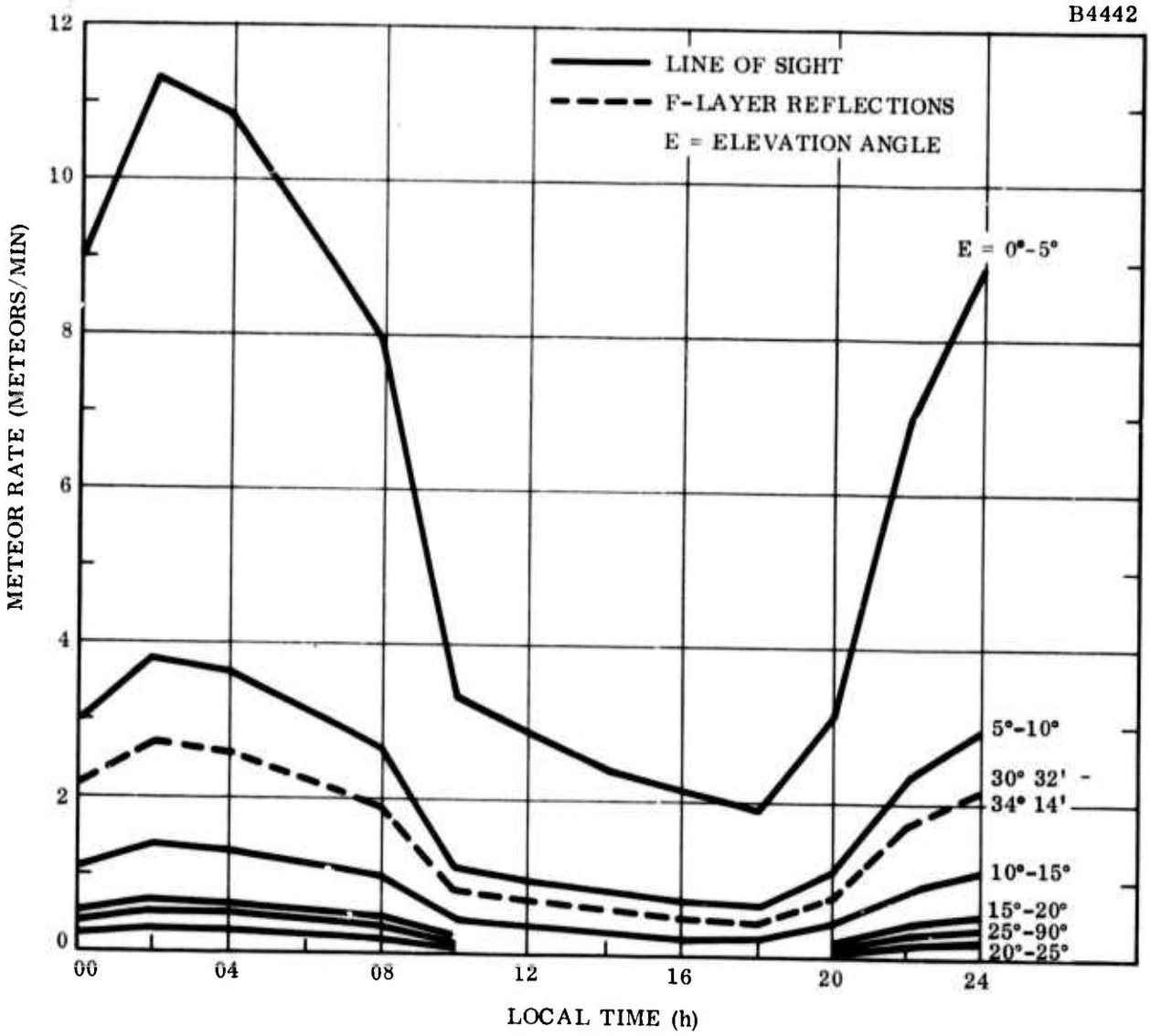

Figure 4-4. Estimated Incremental Rate of Overdense Meteor Echoes in Line-of-Sight at the HF Band Based on Greenhow's and Watkins' Data (1964)

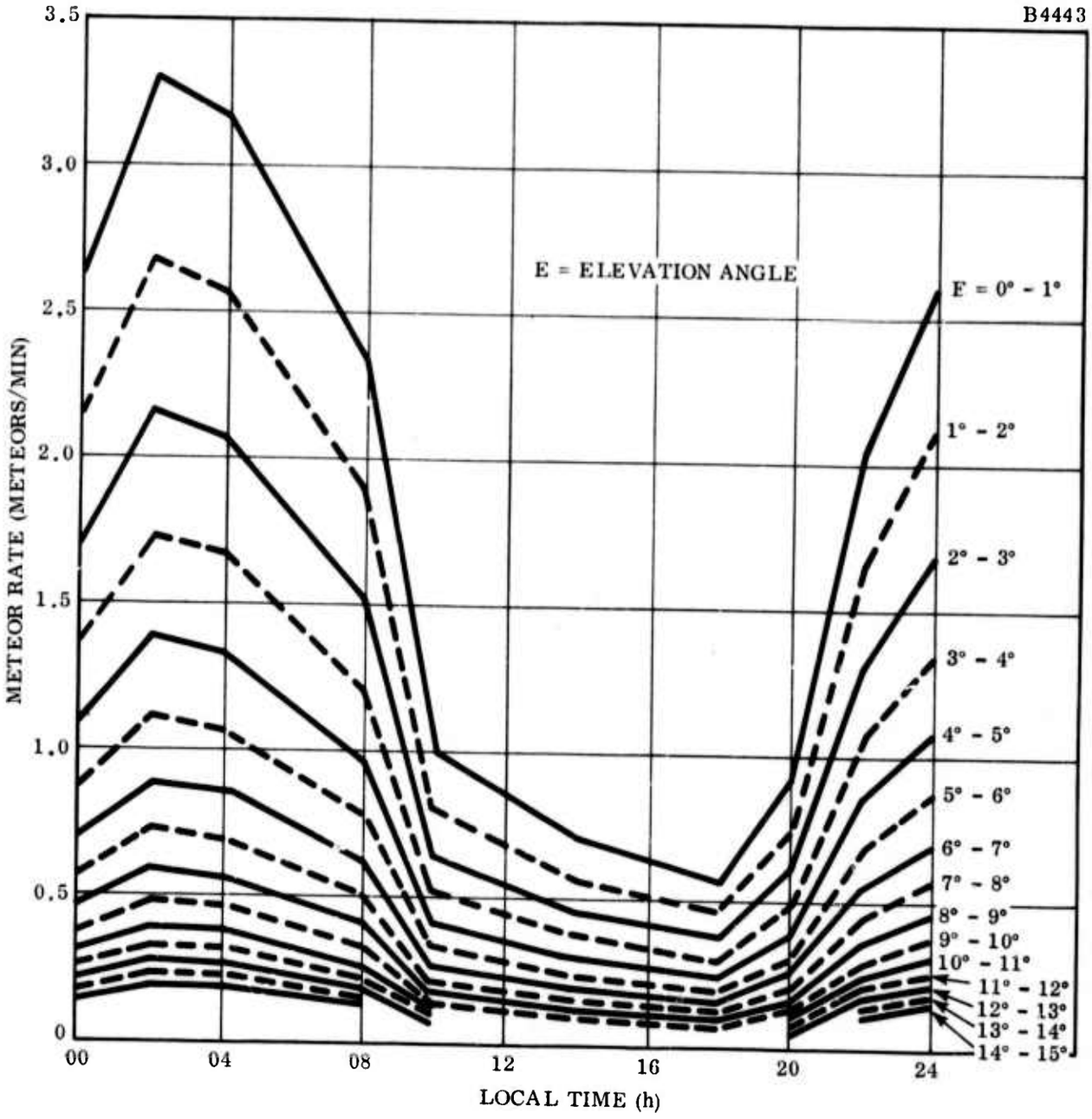

Figure 4-5. Estimated Rate of Overdense Meteor Echoes Between Zero and 15° Elevation Angle in the Line-of-Sight at the HF Band Based on Greenhow's and Watkins' Data (1964)

In addition to the line-of-sight echoes, meteor returns will also appear at over-the-horizon ranges by means of F-layer reflections which, according to Figure 4-2, are specified by the condition $R < R_1 + R_2$. As shown in Appendix F, the surface area at 95 km altitude is 1.334×10^7 km^2 for elevation angle coverage between 0° and 30°32' and 180° azimuthal coverage. This value is approximately 31.76 times greater than the area estimated to be under illumination in the meteor band by Greenhow's and Watkins' equipment. It follows that the over-the-horizon meteor rate will be about 6 times greater than the total line-of-sight rate, i.e., the sum of the direct and F-layer reflection line-of-sight rate. It is reiterated that this conclusion is based on the following assumptions: (1) 350-km F-layer reflection height, (2) 500-nmi skip distance, and (3) 95-km meteor altitude.

The estimated rate of overdense meteor echoes detected at over-the-horizon ranges is presented in Figure 4-6 as a function of elevation angle increments.

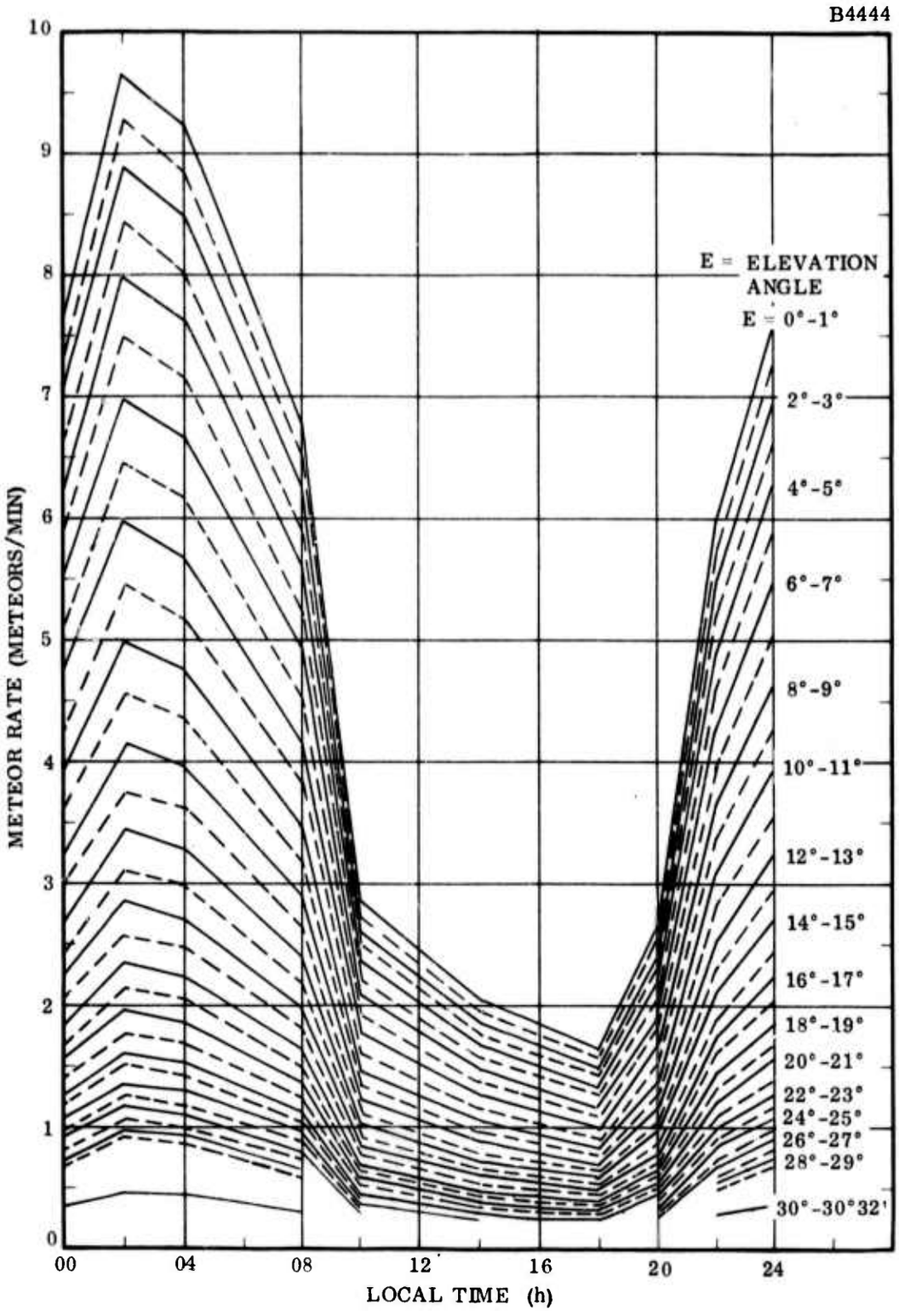

Figure 4-6. Estimated Incremental Rate of Overdense Meteor Echoes After F-Layer Reflection at HF Band Based on Greenhow's and Watkins' Data (1964) at 32 MHz

SECTION V

CONCLUSIONS

Based on the observational data recorded by Greenhow and Watkins at 32 MHz, the median cross-sectional area of overdense meteors, at 6 and 40 MHz, could be on the order of 1.35×10^7 and 2.02×10^6 m^2, respectively. The median time duration at the lower frequency could be as high as 24.2 s while, at the higher frequency, it decreases to about 0.5 s. The extrapolated cross-sectional areas and time durations compare favorably with theoretical estimates.

It is estimated that, for an HF backscatter radar, the maximum number of random overdense meteors appearing in the line-of-sight could be on the order of 21 meteors/min. At over-the-horizon ranges, the maximum overdense meteor rate that could be detected could increase to about 126 meteors/min.

It is postulated from ionospheric wind measurements that, at 6 MHz, the doppler frequency shift encountered on reflection from a meteor trail could be between 2.5 and 4.0 Hz for propagation along the horizon and decreases to zero Hz at the zenith.

The estimated characteristics of the cross-sectional area, time duration and rate of overdense meteor echoes, as described in this report, are based on one set of observational data recorded by Greenhow and Watkins (1964). It would be advantageous to validate these predictions with additional experimental data.

SECTION VI

REFERENCES

Abramowitz, M. and I. A. Stegun, "Handbook of Mathematical Functions with Formulas, Graphs and Mathematical Tables," National Bureau of Standards, Applied Mathematics Series 55, U.S. Government Printing Office, 1965.

Eshleman, V. R., "Meteors and Radio Propagation: Part A-Meteor Ionization Trails, Their Formation and Radio-Echoing Properties," Stanford University Technical Report No. 44, Contract No. N6onr 25132, NR 373 362, February 1955.

Eshleman, V. R., P. B. Gallagher and R. F. Mlodnosky, "Meteor Rate and Radient Studies: Theoretical and Experimental Radio Studies of Meteor Ionization Trails with Application to Radio Propagation by Meteor Reflections," Stanford University Final Report, Contract AF 19(604)-1031, February 1957.

Greenhow, J. S., "Limitations of Radar Techniques for the Study of Meteors," Proceedings of the Symposium on the Astronomy and Physics of Meteors, Smithsonian Contributions to Astrophysics, Vol. 7, pp 5-17, 1963.

Greenhow, J. S. and E. L. Neufeld, "The Diffusion of Ionized Meteor Trails in the Upper Atmosphere," Journal of Atmospheric and Terrestrial Physics, Vol. 6, pp 133-140, March 1959.

Greenhow, J. S. and C. D. Watkins, "The Characteristics of Meteor Trails Observed at a Frequency of 300 Mc/s," Journal of Atmospheric and Terrestrial Physics, Vol. 26, pp 539-558, 1964.

Manning, L. A. and V. R. Eshleman, "Meteors in the Ionosphere," Proceedings of IRE, Vol. 47, pp 186-199, February 1959.

Rao, G. L. N., "Horizontal Drifts and Anisotropy of Irregularities in the Lower Ionosphere - A Review," University of Illinois, Aeronomy Laboratory Report No. 6, June 1965.

APPENDIX A

THE PROBABILITY DENSITY FUNCTION OF THE DOPPLER FREQUENCY SHIFT OF METEOR ECHOES

The reflection of radio waves from a moving object results in a signal returned to a fixed transmitting-receiving system whose frequency differs from the transmitted frequency. This phenomenon referred to as the doppler effect is analytically described by

$$f' = \frac{c - V_r}{c + V_r} f \tag{A-1}$$

where f' is the apparent reflected frequency, f is the transmitted frequency, c is the free space velocity and V_r is the component of the object's velocity in the radial direction.

It can be shown that, for the condition $c >> V_r$, this expression reduces to

$$f_d = -\frac{2V_r}{\lambda} \tag{A-2}$$

where $f_d = f' - f$ and λ is the transmitted wavelength.

When radio waves are incident on meteor trails, the reflected signals undergo a doppler frequency shift, f_d, due to the presence of ionospheric winds. For the meteor echo case, the line-of-sight velocity, V_r, is related to the horizontal wind velocity, V, by the relationship

$$V_r = V_p \cos\beta = V \cos\alpha \cos\beta \tag{A-3}$$

where, according to Figure A-1, V_p is the component of the horizontal wind velocity in the plane containing the radar-antenna beam axis and the vertical through the reflection point.

It is seen from Figure A-1 that the angle β is given by

$$\beta = \frac{\pi}{2} - \gamma \tag{A-4}$$

$$\gamma = \sin^{-1}\left[\frac{r_o}{r_o + h}\cos E\right] \tag{A-5}$$

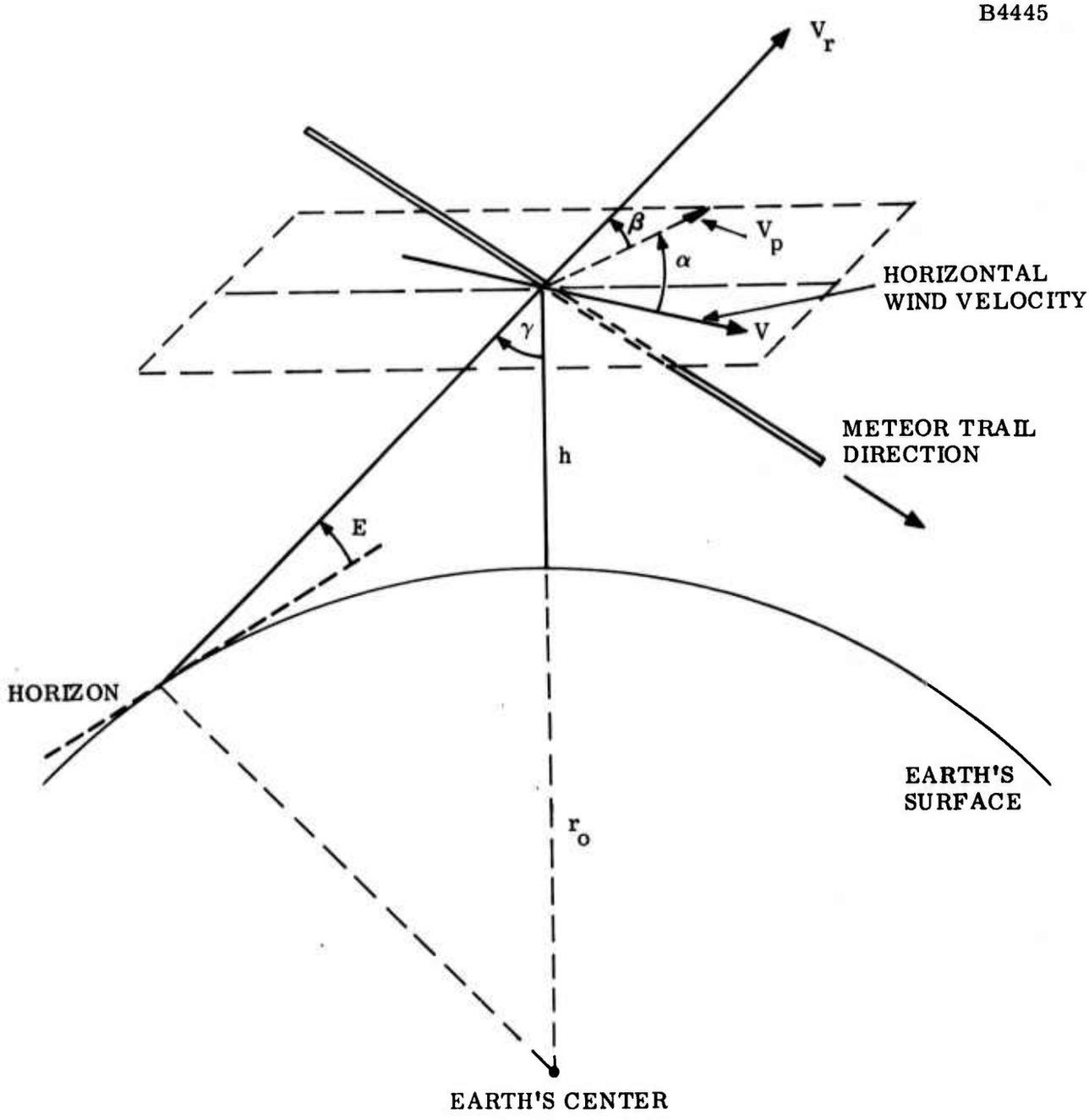

Figure A-1. Meteor Trail and Wind Velocity Geometric Configuration

where γ is the angle between the antenna beam axis and the zenith at the meteor trail - reflection point, r_o is the radius of the earth, E is the elevation angle of the antenna beam and h is the altitude of the reflection point above the earth's surface.

Substituting Equations (A-3), (A-4) and (A-5) in Equation (A-2), there results

$$f_d = AV \cos \alpha \tag{A-6}$$

where

$$A = -\frac{2}{\lambda}\left(\frac{r_o}{r_o + h}\right)\cos E \tag{A-7}$$

In determining the probability density function of f_D, $p(f_D)$, it is assumed that the parameter A is a constant and that the wind velocity, V, and the wind orientation angle, α, are both random independent variables. In other words, the joint probability density function of V and α is therefore the sum of the individual probability density functions.

According to statistical theory, if the probability density function of the variable x is p(x), then for

$$y = f(x) \tag{A-8}$$

the probability density function of y, p(y), is given by

$$p(y)\, dy = p(x)\, dx \tag{A-9}$$

In evaluating $p(f_D)$, it is first assumed that V is also a constant. Thus,

$$p(f_D/V)\, df_D = p(\alpha)\, d\alpha \tag{A-10}$$

According to Equation (A-6)

$$\alpha = \cos^{-1}\left(\frac{f_D}{AV}\right) \tag{A-11}$$

It follows that the differential of α becomes

$$d\alpha = -\frac{1}{A}\,\frac{1}{\left[V^2 - \left(\frac{f_D}{A}\right)^2\right]^{\frac{1}{2}}}\, df_D \tag{A-12}$$

for $V^2 \geq (f_D/A)^2$.

Assuming that the angle α is uniformly distributed in the interval $-\pi \leq \alpha \leq \pi$, then

$$p(\alpha) = \frac{1}{2\pi} \tag{A-13}$$

Since the probability density function $p(f_D/V)$ must be positive and each value of f_D corresponds to two different values of α ($-\alpha$ and $+\alpha$), Equation (A-10) should be written as

$$p(f_D/V) = 2\,p(\alpha) \left| \frac{d\alpha}{df_D} \right| \tag{A-14}$$

Substituting Equations (A-12) and (A-13) in this expression, it follows that

$$p(f_D/V) = \frac{1}{A\pi} \frac{1}{\left[V^2 - \left(\frac{f_D}{A} \right)^2 \right]^{\frac{1}{2}}} \tag{A-15}$$

When considering V as a random variable, the probability density function of f_D can be determined from

$$p(f_D) = \int_{-\infty}^{\infty} p(f_D/V)\, p(V)\, dV \tag{A-16}$$

where $p(V)$ is the probability density function of V.

Substituting Equation (A-15) in this relationship and assuming that V is Rayleigh distributed

$$p(V) = \frac{V}{\psi} \exp\left(- \frac{V^2}{2\psi} \right) \tag{A-17}$$

where

$$\psi = \frac{2}{\pi} (\bar{V})^2 \tag{A-18}$$

and $\bar{V}$ is the mean value of V, it follows that

$$p(f_D) = \frac{1}{A\pi\psi} \int_{f_D/A}^{\infty} \frac{V}{\left[V^2 - \left(\frac{f_D}{A} \right)^2 \right]^{\frac{1}{2}}} \exp\left(- \frac{V^2}{2\psi} \right) dV \tag{A-19}$$

The Rayleigh distribution is discussed in more detail in Appendix B.

To evaluate the integral, it is necessary to change variables. Letting

$$x^2 = V^2 - \left(\frac{f_D}{A}\right)^2 \tag{A-20}$$

$$x\,dx = V\,dV \tag{A-21}$$

Equation (A-19) is modified to

$$p(f_D) = \frac{1}{A\pi\psi} \exp\left[-\frac{1}{2\psi}\left(\frac{f_D}{A}\right)^2\right] \int_0^\infty \exp\left(-\frac{x^2}{2\psi}\right) dx \tag{A-22}$$

Since

$$\int_0^\infty \exp\left(-\frac{x^2}{2\psi}\right) dx = \left(\frac{\pi\psi}{2}\right)^{\frac{1}{2}} \tag{A-23}$$

it follows that

$$p(f_D) = \frac{1}{A\sqrt{2\pi\psi}} \exp\left(-\frac{f_D^2}{2\psi A^2}\right) \tag{A-24}$$

which is a Gaussian distribution. The parameters A and ψ are related to the standard deviation of the Gaussian distribution, σ, by the relationship

$$\sigma = \sqrt{\psi}A \tag{A-25}$$

It is noted that, since the probability density function, $p(f_D)$, is a positive quantity, the absolute value of A, defined by Equation (A-7), must be used.

It follows from Equation (A-18) that the standard deviation of the doppler frequency shift becomes

$$\sigma = 2\left(\frac{2}{\pi}\right)^{\frac{1}{2}} \frac{\overline{V}}{\lambda} \left(\frac{r_o}{r_o + h}\right) \cos E \tag{A-26}$$

APPENDIX B

RAYLEIGH DISTRIBUTION

The probability of occurrence of an ionospheric wind velocity is assumed to be given by the Rayleigh probability distribution law. The probability, p(V) dV, of finding a velocity between V and V + dV, is

$$p(V) = \frac{V}{\psi} \exp\left(-\frac{V^2}{2\psi}\right) \tag{B-1}$$

where V is the velocity at any instant of time and ψ is a constant related to the mean value of V, $\overline{V}$, as given below.

The first and second moments are evaluated from

$$\overline{V} = \int_0^\infty V\, p(V)\, dV \tag{B-2}$$

$$\overline{V} = \left(\frac{\pi\psi}{2}\right)^{\frac{1}{2}} = 1.253\,(\psi)^{\frac{1}{2}} \tag{B-3}$$

and

$$\overline{V^2} = \int_0^\infty V^2\, p(V)\, dV \tag{B-4}$$

$$\overline{V^2} = 2\psi = \frac{4}{\pi}\,\overline{V}^2 = 1.273\,\overline{V}^2 \tag{B-5}$$

The most probable value, V_m, which is the value of V when p(V) is a maximum is

$$V_m = (\psi)^{\frac{1}{2}} = \left(\frac{2}{\pi}\right)^{\frac{1}{2}} \overline{V} = 0.798\,\overline{V} \tag{B-6}$$

The standard deviation, V_σ, which is defined by

$$V_\sigma = \left(\overline{V^2} - \overline{V}^2 \right)^{\frac{1}{2}} \tag{B-7}$$

simplifies to

$$V = \left(\frac{4 - \pi}{\pi} \right)^{\frac{1}{2}} \overline{V} = 0.523 \, \overline{V} \tag{B-8}$$

when substituting Equation (B-5) in Equation (B-7).

The statistics of the Rayleigh distribution can be determined from the cumulative distribution which is described by the integral

$$X = \int_0^V p(V) \, dV \tag{B-9}$$

It can be shown that, on substituting Equation (B-1) in this expression, the integral evaluates to

$$X = 1 - \exp \left(- \frac{V^2}{2\psi} \right) \tag{B-10}$$

Table B-1 lists the decile, quartile and median values of the wind velocity in terms of the mean velocity.

TABLE B-1

STATISTICAL PARAMETERS OF THE RAYLEIGH DISTRIBUTION

Statistical Parameters	Cumulative Distribution (X)	Wind Velocity
Lower Decile	0.10	$V_{LD} = 0.366\ \bar{V}$
Lower Quartile	0.25	$V_{LQ} = 0.605\ \bar{V}$
Median	0.50	$V_{M} = 0.939\ \bar{V}$
Upper Quartile	0.75	$V_{UQ} = 1.329\ \bar{V}$
Upper Decile	0.90	$V_{UD} = 1.712\ \bar{V}$
Standard Deviation	0.1934	$V_{\sigma} = 0.523\ \bar{V}$
Most Probable Value	0.3936	$V_{m} = 0.798\ \bar{V}$

APPENDIX C

SYSTEM SENSITIVITY OF GREENHOW'S AND WATKINS' (1964) RADAR-METEOR EQUIPMENT

The problem is to determine (1) whether Greenhow's and Watkins' (1964) radar equipment could detect overdense meteor trails, and (2) the angular extent over which the overdense trails were detectable.

The minimum signal intensity received by reflections from a meteor trail at the long wavelengths is given by (Eshleman et al., 1957)

$$P_r(\text{min}) = \frac{P_t G_t G_r \lambda^2}{(4\pi)^3 R_o^4} \left(\frac{\sigma_e}{4\pi}\right)^{1/4} (q_{min})^{1/2} \lambda R_o e^{-1/2} \qquad \text{(C-1)}$$

where P_t is the transmitted power, G_t and G_r are the gains of the transmitting and receiving antenna, respectively, λ is the transmitted wavelength, σ_e is the radar cross section of an electron ($\approx 10^{-28}$ m^2), R_o is the perpendicular distance from the radar to the meteor trail and q_{min} is the minimum line density. This expression was derived on the assumption of an expanding cylindrical reflector having a Gaussian distribution of electrons.

According to Table 3-1, $G_t = G_r = 16$ dB (39.81), $P_t = 7$ kW, and $\lambda = 9.375$ m (f = 32 MHz). For an assumed meteor trail reflection height of 95 km and an antenna beam elevation angle of 10°, $R_o = 457$ km.

It is assumed that the system noise, N, is limited by the cosmic noise and that the minimum detectable signal is 10 dB above the external noise level. In other words

$$P_r(\text{min}) = 10 + N \qquad \text{(C-2)}$$

where

$$N = 10 \log KTB \qquad \text{(C-3)}$$

The parameter K is Boltzmann's constant (1.38×10^{-23} watt-sec/deg Kelvin), T is the antenna temperature (15,000° K) and B is the receiver bandwidth which is related to the pulse length, τ, according to $B = 1/\tau$ where $\tau = 140\ \mu$sec. It follows that N = -148.3 dB and $P_r(\text{min}) = -138.3$ dB (1.479×10^{-14}).

Substituting the magnitude of the parameters in Equation (C-1), it is found that the minimum line density which could be detected by the Greenhow and Watkins (1964) radar equipment was approximately 9×10^7 electrons/m. Thus, all the overdense meteor trails were detectable.

To determine the angular extent over which the overdense trails were observed, the minimum line density is taken as 10^{14} electrons/m. Solving for the antenna gain, G, in Equation (C-1), it follows that G = 1.23 (0.9 dB). Thus, overdense meteor echoes should be observed off the main beam axis of the antenna to the point where the gain is about 0.9 dB.

It is assumed that the circular antenna employed by Greenhow and Watkins was uniformly illuminated. Hence, the normalized one-way radiation pattern can be written as

$$S(\gamma) = 2 \frac{J_1 (\pi D \sin \gamma/\lambda)}{(\pi D \sin \gamma/\lambda)} \qquad \text{(C-4)}$$

where $J_1 (\pi D \sin \gamma/\lambda)$ is the Bessel function of the first order, D is the diameter of the aperture (25 m) and γ is the angle off the boresight axis of the antenna.

Since the gain of the antenna was 16 dB (39.81) and the equipment sensitivity was such that overdense meteors could be detected as far down as 0.9 dB (1.23), the normalized beam pattern becomes (1.23/39.81) = 0.0309. It follows from Equation (C-4) that

$$\frac{J_1 (\pi D \sin \gamma/\lambda)}{(\pi D \sin \gamma/\lambda)} = 0.0155 \qquad \text{(C-5)}$$

According to the tabulations of the Bessel functions of Abramowitz and Stegun (1965), for this value of the Bessel function

$$\frac{\pi D \sin \gamma}{\lambda} = 3.6925 \qquad \text{(C-6)}$$

Thus, $\sin \gamma = 0.44076$ and $\gamma = 26.15°$.

APPENDIX D

OVERDENSE METEOR ECHO GEOMETRY OF GREENHOW AND WATKINS (1964)

In determining the spatial extent in the ionosphere of the overdense meteor echoes observed by Greenhow and Watkins (1964), it is assumed that the area formed by the intersection of the antenna beam with the meteor band can be represented by

$$A_{GW} = A_s + A_r \tag{D-1}$$

where, as shown in Figure D-1, A_s is approximated by a semicircle and A_r by a rectangle. It should be evident that

$$A_s = \frac{1}{2} \pi R_m^2 \gamma^2 \csc \psi \tag{D-2}$$

$$A_r = 2 R_m^2 E \gamma \csc \psi \tag{D-3}$$

where R_m is the distance from the radar to the meteor band, E is the elevation angle of the antenna beam and γ is the angle off the antenna beam axis encompassing the region of the overdense echoes.

The angle ψ which is the complement of the incidence angle, e, at the meteor band is given by

$$\psi = 90° - e = 90° - \sin^{-1}\left[\frac{r_o}{r_o + h_m} \cos E\right] \tag{D-4}$$

where r_o is the radius of the earth (6371 km) and h_m is the meteor altitude.

For $E = 10°$ and $h_m = 95$ km, it is found that $\psi = 13.99°$. Noting that $R_o = 457$ km and $\gamma = 26.15°$, as derived in Appendix C, the areas A_r and A_s evaluate to 1.376×10^5 km and 2.827×10^5 km^2, respectively. It follows that $A_{GW} = 4.203 \times 10^5$ km^2.

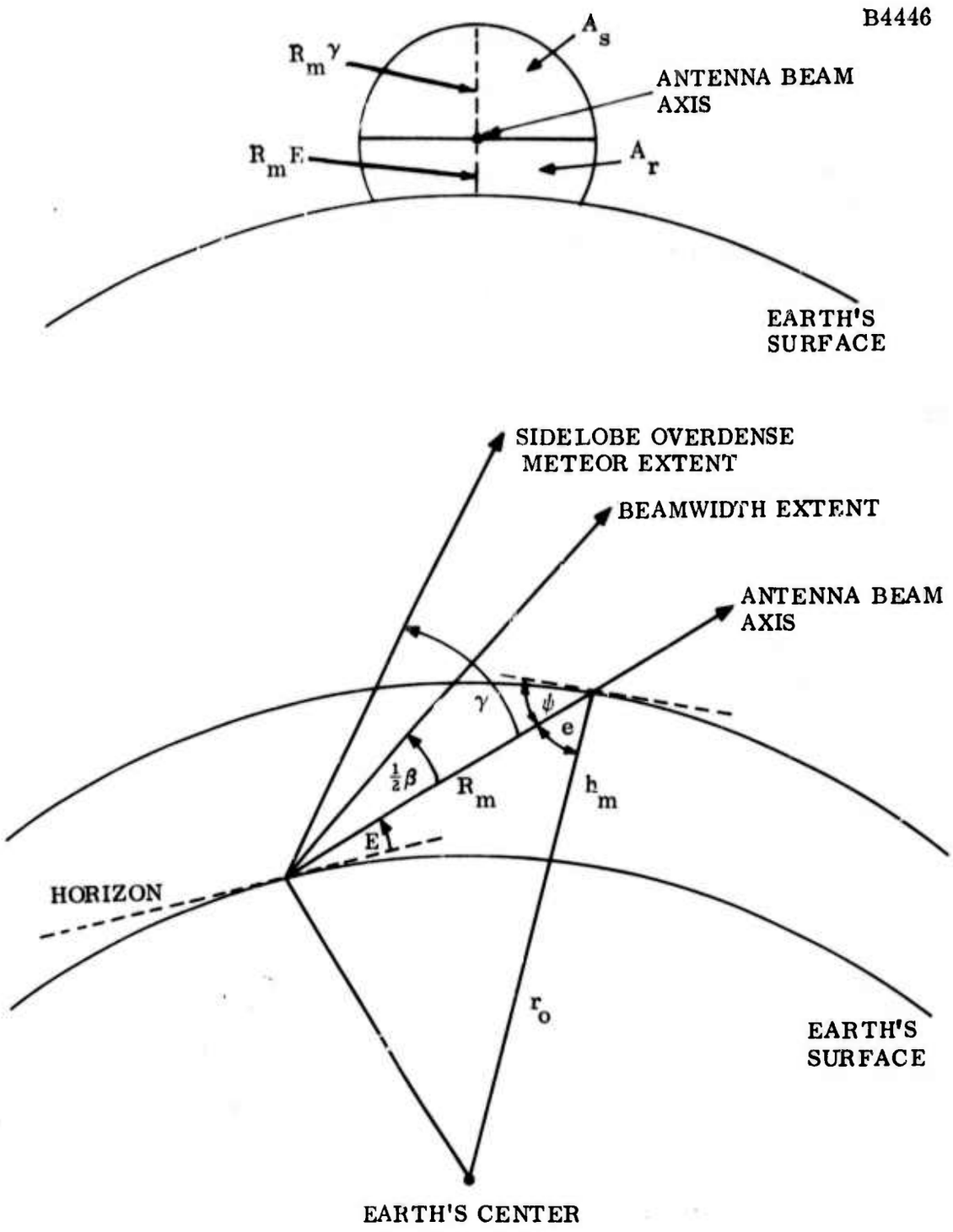

Figure D-1. Geometry of Overdense Meteor Echoes Observed by Greenhow and Watkins (1964)

APPENDIX E

METEOR ECHO GEOMETRY IN THE DIRECT LINE-OF-SIGHT OF AN HF BACKSCATTER RADAR

It is assumed that overdense meteor echoes can be detected at all azimuth and elevation angles in the antenna sidelobes of an HF backscatter radar. Thus, the entire region above the horizon at a radar site must be considered in determining the area in the meteor band under radar illumination.

According to Figure E-1, the surface area of the ionosphere above the horizon, A_m, is given by

$$A_m = A_1 - A_2 \tag{E-1}$$

where A_1 is the surface area of a hemisphere

$$A_1 = 2\pi (r_o + h_m)^2 \tag{E-2}$$

and A_2 is the area of the curved surface of a spherical segment

$$A_2 = 2\pi (r_o + h_m) r_o \tag{E-3}$$

The parameter r_o is the radius of the earth and h_m is the altitude to the meteor band.

Substituting Equations (E-2) and (E-3) in Equation (E-1) and taking into account the fact that only one-half the azimuthal spread would be effective in the detection of the overdense meteor trails because of "holes" in the sidelobe antenna pattern, it follows that the area under surveillance becomes

$$A_m = \pi (r_o + h_m) h_m \tag{E-4}$$

For $r_o = 6371$ km and $h_m = 95$ km, $A_m = 1.9298 \times 10^6$ km^2.

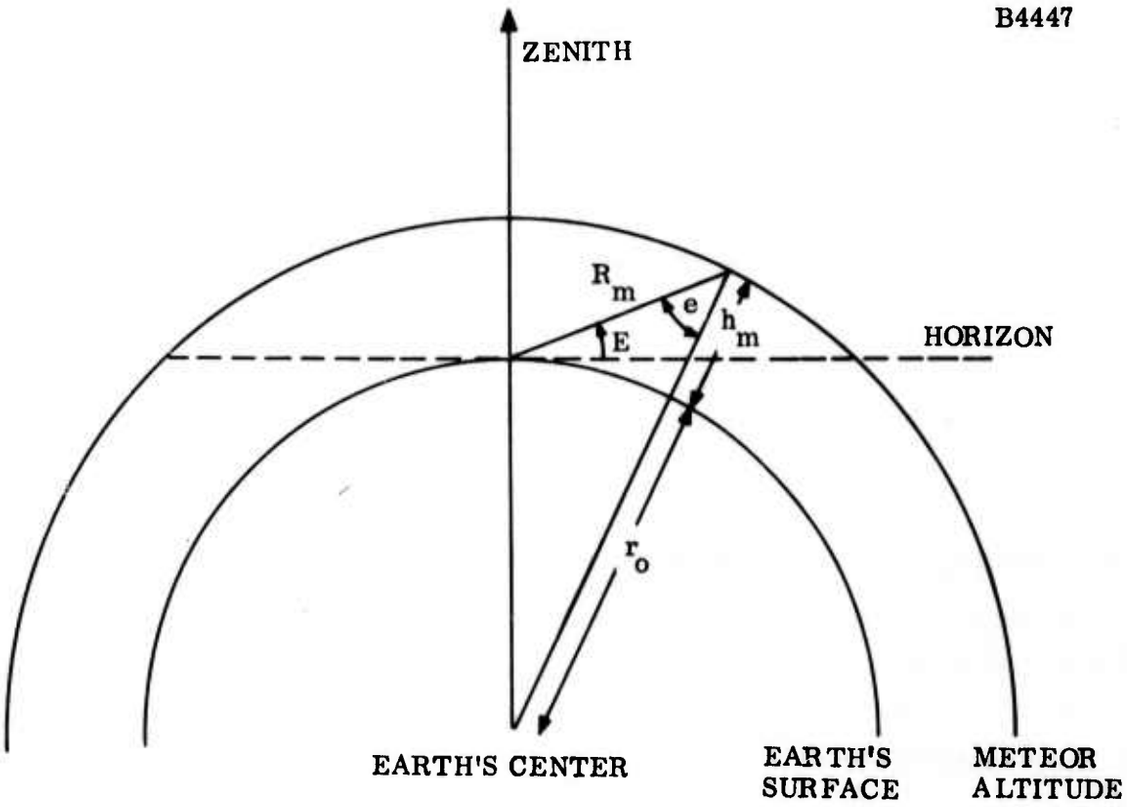

Figure E-1. Meteor Band Illumination Area for Direct Line-of-Sight Geometry

APPENDIX F

METEOR ECHO GEOMETRY FOR F-LAYER REFLECTIONS

HF transmissions undergoing F-layer propagation can be reflected by meteor trails which could appear at the same range as the line-of-sight meteor echoes. For the ranges of the line-of-sight and F-layer reflected meteor echoes to be coincident, the condition that must be satisfied is $R \geq R_1 + R_2$ where, according to Figure F-1, R is the radar-horizon range to the meteor trail, R_1 is the range to the F-layer reflection point and R_2 is the range from the F-layer reflection point to the meteor trail.

The maximum elevation angle at which F-layer reflected meteor echoes appear at the same range as the line-of-sight echoes can be determined from the expressions

$$E_{max} = \cos^{-1}\left[\frac{r_o + h_F}{R_1} \sin(\theta''_1 + \theta''_2)\right] \tag{F-1}$$

$$R_1 = \left[r_o^2 + (r_o + h_F)^2 - 2\, r_o\, (r_o + h_F) \cos(\theta''_1 + \theta''_2)\right]^{1/2} \tag{F-2}$$

$$\theta''_1 + \theta''_2 = \frac{d}{2\, r_o} \tag{F-3}$$

where r_o is the radius of the earth, h_F is F-layer reflection altitude and d is the skip distance. For d = 500 nmi (926.59 km), h_F = 350 km and r_o = 6371 km, $\theta''_1 + \theta''_2 = 4.167°$, R_1 = 590.63 km and $E_{max} = 34.222°$ (34°13').

The earth's central angle, θ''_1, can be determined utilizing the law of sines. It can be readily shown from Figure F-1 that

$$\theta''_1 = 90° - E_{max} - \sin^{-1}\left[\frac{r_o}{r_o + h_m} \cos E_{max}\right] \tag{F-4}$$

where h_m is the meteor altitude. Assuming h_m = 95 km, $\theta''_1 = 1.219°$ and $\theta''_2 = \theta''_3 = 2.948°$.

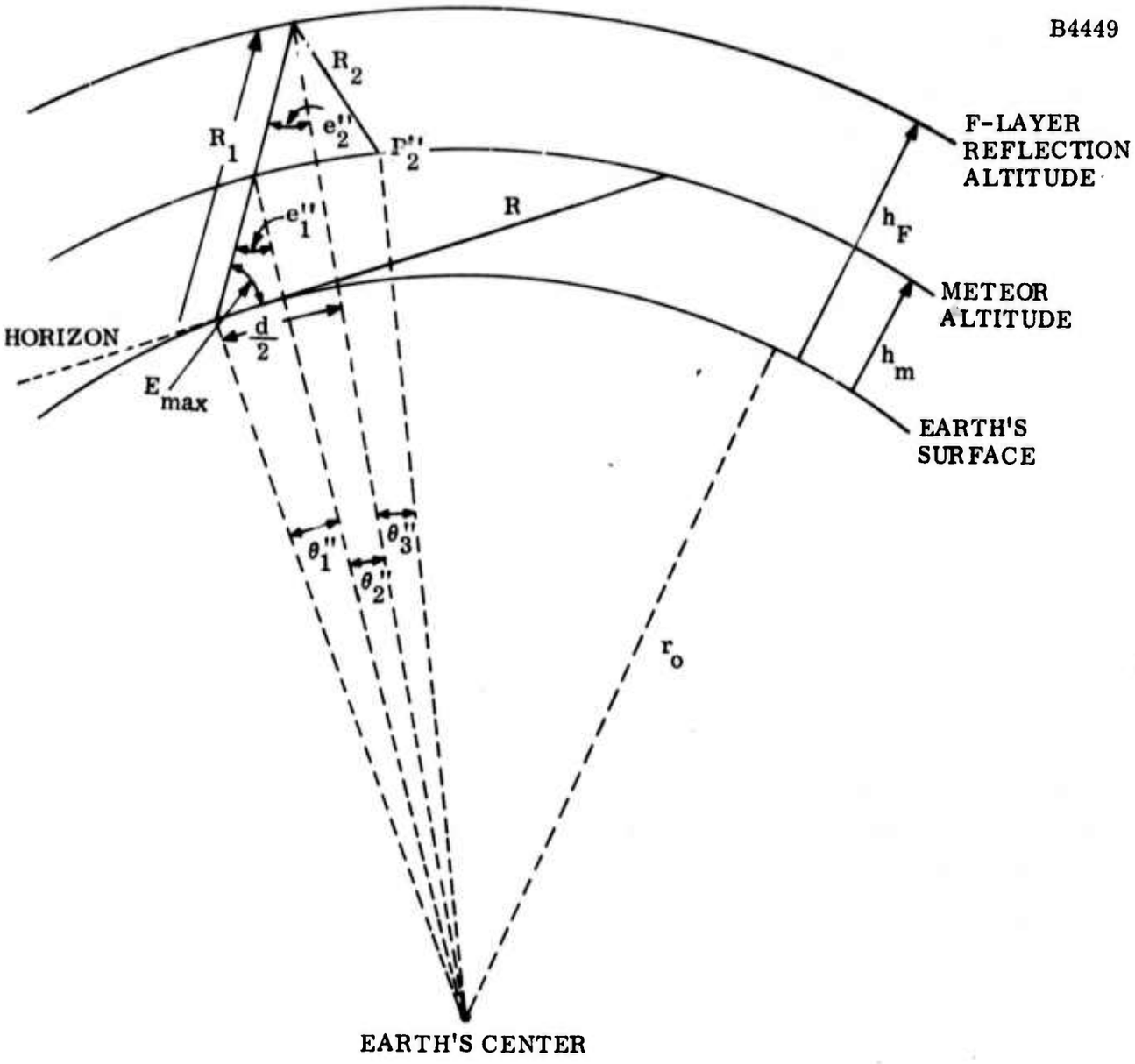

Figure F-1. Meteor Echo Geometry for F-Layer Reflections - Maximum Elevation Angle

The minimum elevation angle is the angle which satisfies the range condition $R = R_1 + R_2$ and can be deduced by an iterative process. The first step in the solution of the problem is to assume a value for E_{min}, depicted in Figure F-2, and then to apply it to the following calculations.

$$e'_2 = \sin^{-1}\left[\frac{r_o}{r_o + h_F} \cos E_{min}\right] \tag{F-5}$$

$$e'_1 = \sin^{-1}\left[\frac{r_o}{r_o + h_m} \cos E_{min}\right] \tag{F-6}$$

$$\theta'_1 + \theta'_2 = 90° - (e'_2 + E_{min}) \tag{F-7}$$

$$\theta'_1 = 90° - (e'_1 + E_{min}) \tag{F-8}$$

$$\theta'_2 = \theta'_3 \tag{F-9}$$

$$R_1 = (r_o + h_F) \frac{\sin(\theta'_1 + \theta'_2)}{\cos E_{min}} \tag{F-10}$$

$$R_1 - R_2 = (r_o + h_m) \frac{\sin \theta'_1}{\cos E_{min}} \tag{F-11}$$

$$R = 2R_1 - (R_1 - R_2) = R_1 + R_2 \tag{F-12}$$

$$R = \left[(r_o + h_m)^2 - r_o^2\right]^{1/2} \tag{F-13}$$

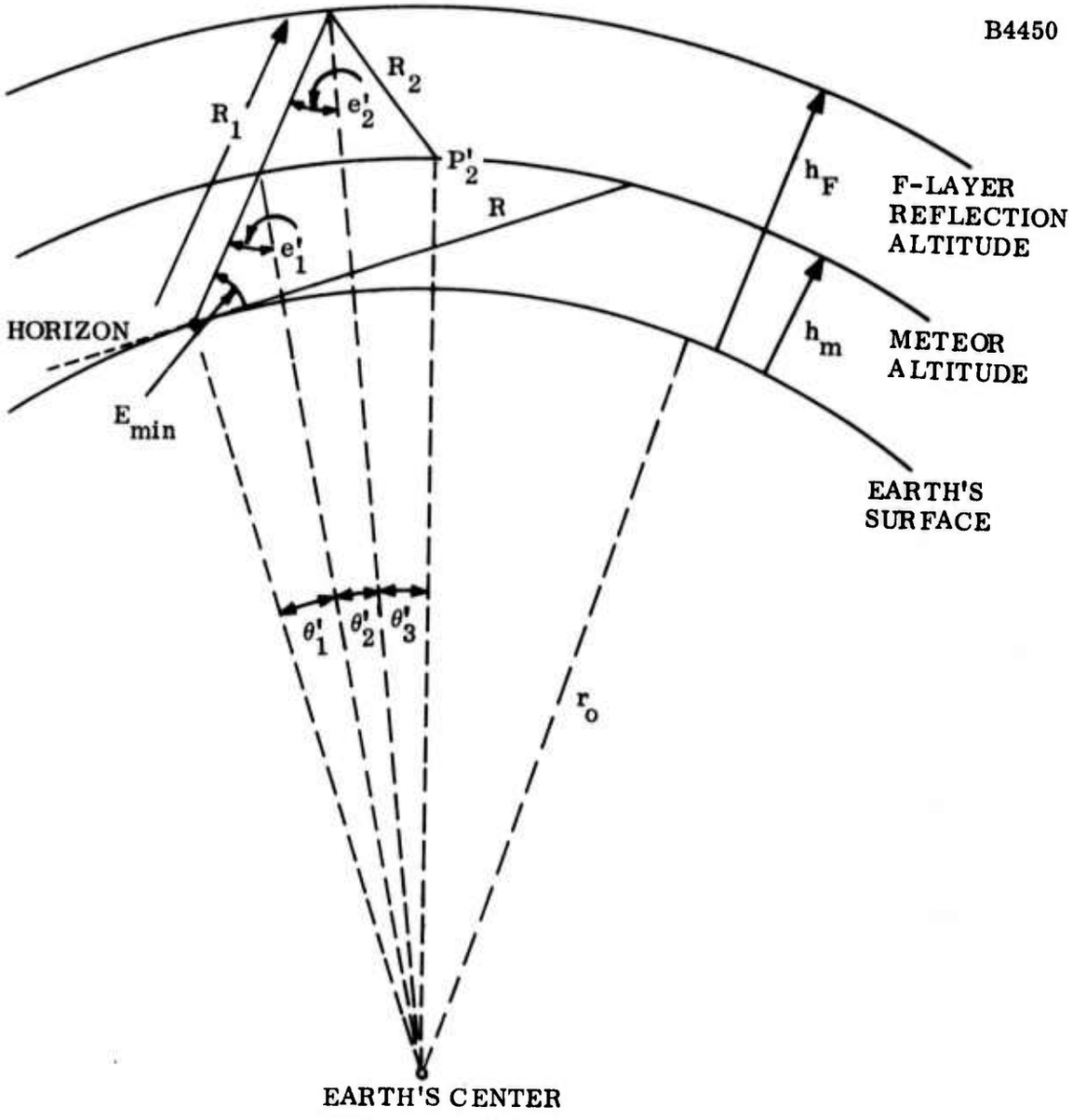

Figure F-2. Meteor Echo Geometry for F-Layer Reflections - Minimum Elevation Angle

For h_m = 95 km, R = 1104.32 km. Assuming h_F = 350 km, it is found that E_{min} = 30.535° (30°32'), θ'_1 = 1.400°, θ'_2 = 3.338°, R_1 = 644.06 km, $R_1 - R_2$ = 183.30 km and $R_1 + R_2$ = 1104.82 km which compares favorably with the line-of-sight horizon range of 1104.32 km.

The central angle, ϵ, specified by the arc, $\overset{\frown}{P''_2 P'_2}$, shown in Figure F-3 which is a simplified composite of Figures F-1 and F-2, can be determined from

$$\epsilon = (\theta'_1 + \theta'_2 + \theta'_3) - (\theta''_1 + \theta''_2 + \theta''_3) \tag{F-14}$$

Since $(\theta'_1 + \theta'_2 + \theta'_3) = 8.076°$ and $(\theta''_1 + \theta''_2 + \theta''_3) = 7.115°$, it follows that $\epsilon = 0.961°$.

As discussed in Appendix E, the surface area in the meteor band encompassed by the angle, ϵ, can be deduced from the relationship

$$A = 2\pi (r_o + h_m)(z_2 - z_1) \tag{F-15}$$

where, according to Figure F-4,

$$z_2 = (r_o + h_m) \sin (\epsilon + \phi) \tag{F-16}$$

$$z_1 = (r_o + h_m) \sin \phi \tag{F-17}$$

Since

$$\phi = 90° - (\epsilon + \theta''_1 + \theta''_2 + \theta''_3) \tag{F-18}$$

it follows that the surface area can be written as

$$A = \pi (r_o + h_m)^2 \left[\cos (\theta''_1 + \theta''_2 + \theta''_3) - \cos (\theta''_1 + \theta''_2 + \theta''_3 + \epsilon)\right] \tag{F-19}$$

It is noted that this relationship is based on the supposition that an azimuthal spread of 180° is only effective in detecting the overdense meteor echoes.

For h_m = 95 km, $(\theta''_1 + \theta''_2 + \theta''_3) = 7.115°$ and $(\theta''_1 + \theta''_2 + \theta''_3 + \epsilon) = 8.076°$, the surface area evaluates to 2.91×10^5 km^2.

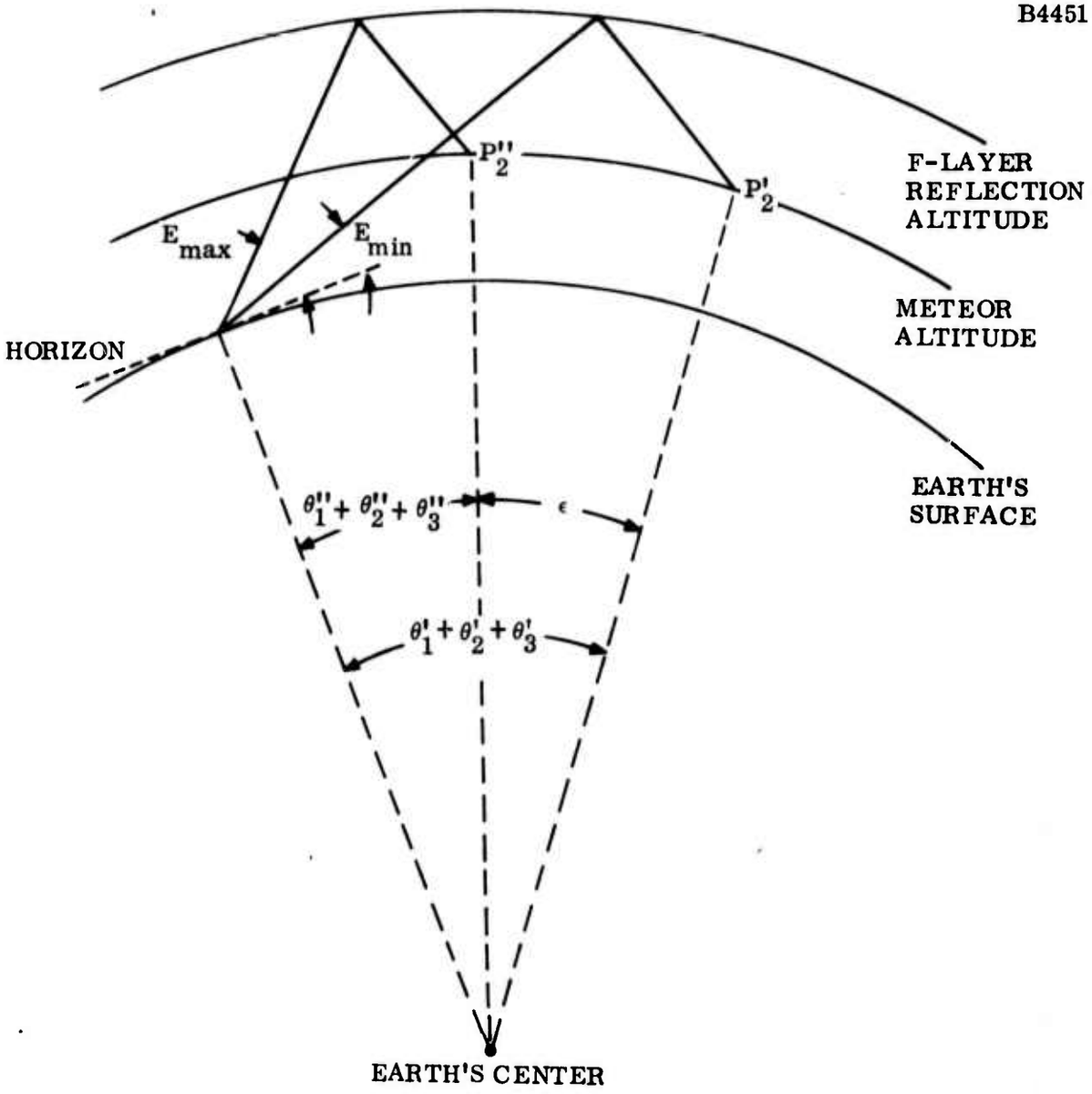

Figure F-3. Meteor Echo Geometry for F-Layer Reflections - Composite

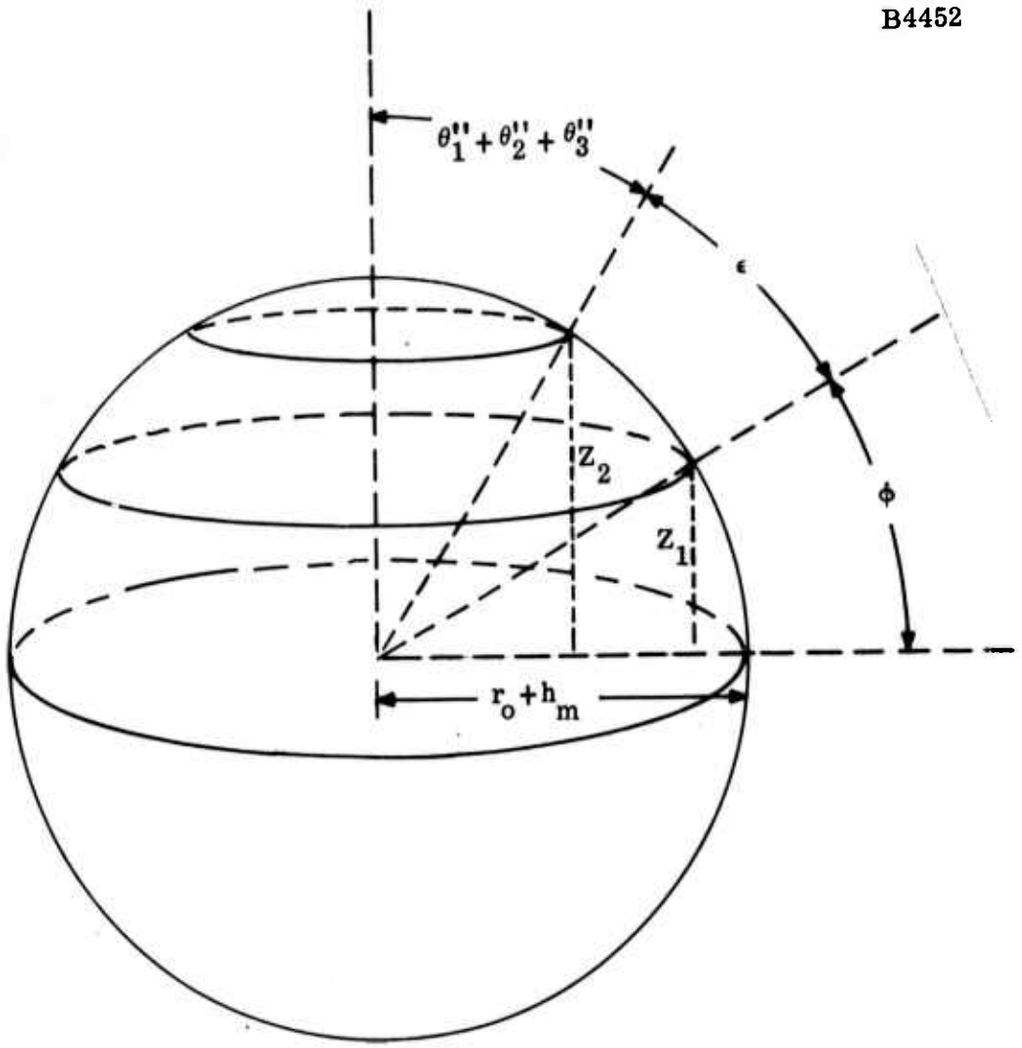

Figure F-4. Meteor Band Illumination Area for F-Layer Reflection Geometry

For HF transmissions reflected from the F-layer, meteor echoes could appear at ranges greater than the line-of-sight meteor echo range. The condition that must be satisfied for this to occur is $R < R_1 + R_2$ where R, R_1 and R_2 are the ranges depicted in Figure F-1. The overdense meteor echo rate at over-the-horizon ranges can be readily determined from the area illuminated in the meteor band.

The surface area at the meteor band illuminated within any two elevation angles, $E_2 - E_1$, can be derived similar to the procedure employed to describe the area between the maximum and minimum elevation angles. Equations (F-14) and (F-19) are also valid for the general case. The relationships that must be modified are those defining the angles θ''_1, θ''_2, θ'_1 and θ'_2.

By replacing E_{max} by the angle E_2 and E_{min} by E_1, θ''_1 given by Equation (F-4) becomes

$$\theta''_1 = 90° - E_2 - \sin^{-1}\left[\frac{r_o}{r_o + h_m}\cos E_2\right] \qquad \text{(F-20)}$$

while θ''_2 is written in the form

$$\theta''_1 + \theta''_2 = 90° - E_2 - \sin^{-1}\left[\frac{r_o}{r_o + h_F}\cos E_2\right] \qquad \text{(F-21)}$$

The angle θ'_1 is given by

$$\theta'_1 = 90° - E_1 - \sin^{-1}\left[\frac{r_o}{r_o + h_m}\cos E_1\right] \qquad \text{(F-22)}$$

while θ'_2 is defined by

$$\theta'_1 + \theta'_2 = 90° - E_1 - \sin^{-1}\left[\frac{r_o}{r_o + h_F}\cos E_1\right] \qquad \text{(F-23)}$$

It is noted that $\theta'_2 = \theta'_3$ and $\theta''_2 = \theta''_3$.

The surface area encompassed between the elevation angles of 0° and 30.535° (E_{min}) can be calculated utilizing the above relationships. For $E_2 = 30.535°$, $\theta''_1 = 1.400°$, $\theta''_2 = 3.338°$ and $(\theta''_1 + \theta''_2 + \theta''_3) = 8.076°$ while for $E_1 = 0°$, $\theta'_1 = 9.834°$, $\theta'_2 = 8.738°$, $(\theta'_1 + \theta'_2 + \theta'_3) = 27.310°$ and $\epsilon = 19.234°$. The surface area thus evaluates to 1.334×10^7 km^2.

APPENDIX G

INCREMENTAL METEOR BAND ILLUMINATION AREA FOR DIRECT LINE-OF-SIGHT GEOMETRY

The area in the meteor band illuminated within the incremental elevation angle, $E_2 - E_1$ depicted in Figure G-1, can be determined utilizing the geometric concepts presented in Appendix E.

The general expression for the surface area of a zone of a sphere is given by

$$A_{h1} = 2\pi (r_o + h_m) (r_o + h_1) \tag{G-1}$$

where A_{h1} is the surface area associated with the zonal height, $r_o + h_1$, r_o is the radius of the earth and h_m is the meteor altitude.

Similarly, for the zonal height, $r_o + h_2$, the surface area, A_{h2}, is simply

$$A_{h2} = 2\pi (r_o + h_m) (r_o + h_2) \tag{G-2}$$

It follows that the incremental surface area

$$A = A_{h2} - A_{h1} \tag{G-3}$$

can be represented by the relationship

$$A = 2\pi (r_o + h_m) (h_2 - h_1) \tag{G-4}$$

It is evident from Figure G-1 that

$$h_1 = R_{m1} \sin E_1 \tag{G-5}$$

$$h_2 = R_{m2} \sin E_2 \tag{G-6}$$

Since from the law of sines

$$R_{m1} = (r_o + h_m) \frac{\sin \theta_1}{\cos E_1} \tag{G-7}$$

and noting that

$$\theta_1 = 90° - (E_1 + e_1) \tag{G-8}$$

and

$$\sin e_1 = \left(\frac{r_o}{r_o + h_m}\right) \cos E_1 \tag{G-9}$$

it follows that R_{m1} can be written as

$$R_{m1} = (r_o + h_m) \left\{ \cos \left[\sin^{-1} \left(\frac{r_o}{r_o + h_m} \cos E_1 \right) \right] - \left(\frac{r_o}{r_o + h_m} \right) \sin E_1 \right\} \tag{G-10}$$

Similarly, it can be shown that

$$R_{m2} = (r_o + h_m) \left\{ \cos \left[\sin^{-1} \left(\frac{r_o}{r_o + h_m} \cos E_2 \right) \right] - \left(\frac{r_o}{r_o + h_m} \right) \sin E_2 \right\} \tag{G-11}$$

Substituting Equations (G-5), (G-6), (G-10) and (G-11) in Equation (G-4), there result

$$A = 2\pi (r_o + h_m)^2 \left\{ \cos \left[\sin^{-1} \left(\frac{r_o}{r_o + h_m} \cos E_2 \right) \right] \sin E_2 \right.$$

$$\left. - \cos \left[\sin^{-1} \left(\frac{r_o}{r_o + h_m} \cos E_1 \right) \right] \sin E_1 - \left(\frac{r_o}{r_o + h_m} \right) (\sin^2 E_2 - \sin^2 E_1) \right\} \tag{G-12}$$

It is noted that this expression is applicable for the condition in which an antenna beam and sidelobes completely illuminate the entire meteor band. When assuming that there are holes in the sidelobe antenna pattern, as considered in this study, the surface area given by Equation (G-12) is reduced by a factor of one-half.

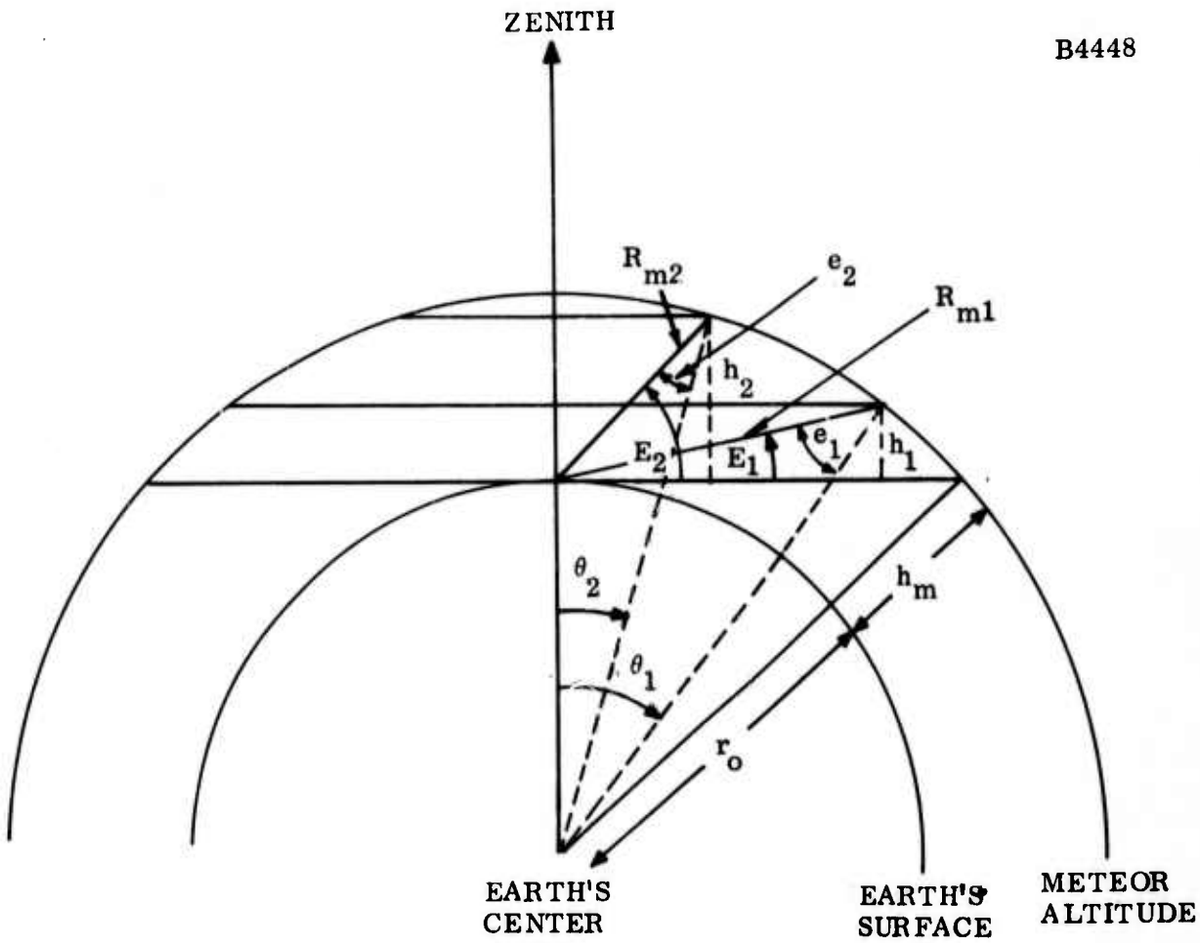

Figure G-1. Incremental Elevation Angle - Meteor Band Illumination Area For Direct Line-of-Sight Geometry